When two become one

an insight into 2D conductive oxide interfaces

Pryds, Nini; Esposito, Vincenzo

Published in:
Journal of Electroceramics

Link to article, DOI:
10.1007/s10832-016-0051-0

Publication date:
2017

Document Version
Peer reviewed version

When two become one: An insight into 2D conductive oxide interfaces

Nini Pryds and Vincenzo Esposito
Department of Energy Conversion and Storage, Technical University of Denmark, Risø DTU Campus, Frederiksborgvej 399, 4000 Roskilde, Denmark

Abstract

Recent progress has led to conductance confinement at the interface of complex oxide heterostructures thereby providing new opportunities to explore nano-electronic as well as nano-ionic devices. In this paper we describe how interfacial contiguity between materials can trigger redox reaction inducing metallic conductivity along the interface of $SrTiO_3$-based heterostructures and create new types of 2DEG at the hetero-interface, where electron mobility enhancement is of more than one order of magnitude higher than those of hitherto investigated perovskite-type interfaces. In the same frame, our recent results on examining the strain effects at interfaces demonstrate that by controlling the growth of hetero-epitaxial thin films, it becomes possible to obtain ionic or electronic conductive films with superior properties. We also present a novel concept which uncovers a large variety of possible technological perspectives for materials design using multi-layered heterostructures of ionic conductors. These findings can pave the way for all-oxide electronic and ionic devices.

From bulk to interfaces

Surfaces and interfaces have in the recent decades played an important role within physics and chemistry of condensed matter. A solid interface is defined as an atomic layer which separate two solids when they brought into close contact with each other. Some of the most important properties in todays advanced materials stem from the functionality of the interfaces, when the interface is formed between two solid materials. These interfaces exhibit properties that are far from the pristine materials and they can be seen as building blocks that allow creating materials without similar bulk analogues. A highly promising class of such materials, that is proving increasingly interesting, is the complex oxides [1-4]. The interest in complex oxides is owing to their unique interaction between the spin, lattice, charge, and orbital degrees of freedom a variety of novel phenomena observed in these compounds. During the last 20 years, oxides have been a subject of intense research as this class of materials exhibits an exceptionally broad range of remarkable properties. Chemically, oxides range from being extremely inert to very reactive allowing for application in as different areas as self-healing corrosion protection layers [5] and chemically active catalysts [6]. Electronically, oxides span the full spectra composed of insulators with wide band-gaps [7] or

large dielectric constants [8], high temperature superconductors [9], metallic conductors [10], ionic conductors [11] and semiconductors [12]. Ferroelectricity [13], piezoelectricity [14], flexoelectricity [15] and spin polarized electron transport [16] have likewise been reported in oxides. A vast variety of magnetic properties is also observed including ferromagnetism exhibiting high saturation magnetism [17], tunable transition temperature between different magnetic phases [18], colossal magnetoresistance [19] and magnetostriction [20].

The architecture of oxides thin films can formally be divided into two classes: *single film* oxide material and *heterostructures*, containing one or several types of oxides. While the former has been thoroughly investigated for a broad range of oxides thin films, much research has yet to be performed on the latter systems in order to unravel the wide range of possibilities and functionality behind the oxide heterostructures but also on a fundamental level. Particularly challenging in doing so is the fact that the properties of the oxides often are critically dependent on the structure, microstructure, stoichiometry, amount of dopants and defects, which requires that both the heterostructure and the substrates are of superior quality. The development in substrate growth and deposition methods within the last 20 years has enabled the fabrication of oxide heterostructures with a quality reaching the level obtainable with the current traditional semiconductor technology. Since oxide multilayers are far more difficult to grow than the conventional semiconductor heterostructures, development in oxide electronics has been hindered for many years. Intensive efforts over the past two decades to improve the condition and the growth quality of oxide crystals have led to significant progress in the growth of oxide multilayers. Key steps in this direction were the ability to control the oxide substrates at well-defined surface atomic layer, the advanced of pulsed-laser deposition (PLD) and the development tools to control the growth of the layer on an atomic scale [21]. In summary, interfaces of oxide materials have display an astonishing variety of electronic and ionic phenomena some of which will be discussed in this review. The review is divided into two main parts. The first part gives details of electronic behaviour of oxide heterostructure and this is followed by the second part which describes the latest trend and findings for oxygen ionic conduction in complex oxide heterostructures.

1. Electronic complex oxide heterostructures

When H. Kroemer (Nobel Prize in 2000) coined the phrase "the interface is the device", he was referring to the working principle of the semiconductor transistors, which has transformed everyday life [22]. Twelve years later an editorial in *Nature Materials* with the title "The interface is still the device" [23] drew attention to the fact that we are on the threshold of a similar breakthrough, this time arising from interfaces and heterostructures of oxide-based materials. The interest in these interface transition-metal oxides has motivated considerable

amount of research in epitaxial growth of oxide heterojunctions and artificial layered oxides. The electronic properties of transition-metal oxides are determined by strong correlations which involve hybridized oxygen *p* and transition-metal *d* orbitals. Transition metals are strongly correlated-electron systems which are very sensitive to the orbitals at the Fermi energy and thereby exceptionally sensitive to exterior influence such as doping and strain. The interfaces in such type of materials can therefore lead to a new physics and the generation of electronic devices with properties well beyond those we experience today. Oxide heterostructures introduce a variety of extraordinary properties, such as superconductivity [24], thermoelectricity [25], ionic conductivity [26] and ferromagnetism [27]. One of the cardinal questions is whether conducting oxide interfaces could become the cornerstone of oxide electronics? This is a question which is very difficult and not straightforward to answer. The reason is that currently these oxide interfaces are characterized by higher carrier densities and also much shorter electron mean free path than conventional semiconductor interfaces. These are the current limiting factors of using these materials in electronic devices. What one hope to achieve is to be able to emulate the achievements of semiconductor materials researchers who have over the past few decades learned how to engineer the electronic properties of epitaxially grown semiconductor materials by exploiting lattice-matching strains and modulation of doping. Owing to the greater sensitivity of their electronic properties and because of the wider range of phenomena that can be observed in these interfaces, the implications for basic physics and technological application using oxide heterostructures are likely to be enormous.

In 2004 at Bell Lab a surprising metallic state was found at the interface between the large band gap insulator $LaAlO_3$ (LAO), epitaxially grown on an insulating STO substrate (see Fig. 1) [28]. This initiated a large research activity, and since then many other heterostructures have been found to exhibit interfacial 2DEGs with intriguing properties, such as superconductivity [24], ferromagnetism [27], field-induced metal-insulator transition [29], and optical sensitivity [30]. The mechanism underlying the two-dimensional electron gas (2DEG) at the interface between two insulating oxides of LAO and STO is still unclear and under a debate. Although,

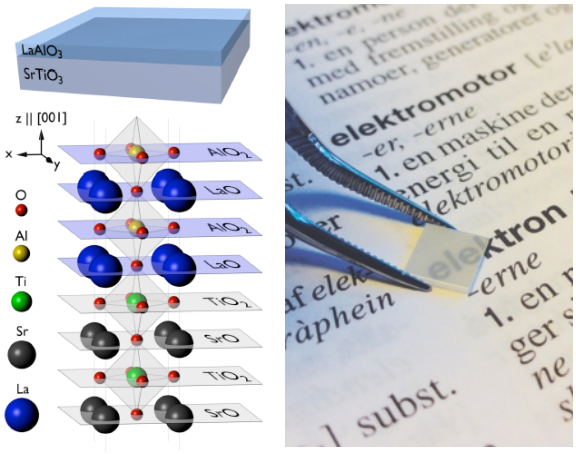

Fig. 1 The figure to the left is the electronic structure of the STO and LAO. To the right, transparent STO substrate deposited on the top with LAO using Pulsed Laser Deposition

several arguments have been shown to favour the "polar catastrophe model" [31], the mechanism is not yet settled. This is maybe because it is very much depended on the materials system and fabrication conditions. The reason for the creation of complex oxide 2DEGs can mainly be divided into three groups (see also Fig. 2):

(1) Electronic reconstruction (Fig. 2a) resulting from the polar discontinuity at a polar−nonpolar oxide interface. Such interfacial polar discontinuity requires the presence of a polar oxide, which consists of alternating positively and negatively charged sublayers, epitaxially grown on nonpolar $SrTiO_3$, such as $LaAlO_3/SrTiO_3$ (LAO/STO) [31];

(2) Creation of oxygen vacancies at the bare STO surface or in STO-based heterostructures having interfacial redox reactions, such as vacuum cleaved STO or the system of amorphous-$LaAlO_3/SrTiO_3$ (a-LAO/STO) [32] (Fig. 2b);

(3) 2DEGs by delta doping of STO, typically sandwiching a Nb- or La-doped STO thin layer between two non-doped STO layers [33] (see also Fig. 2c).

Among these, the polarity issue, particularly in the LAO/STO system, has drawn the most attention due to the possibility of an intrinsic doping of STO by electronic reconstruction without the typical disorder caused by chemical doping.

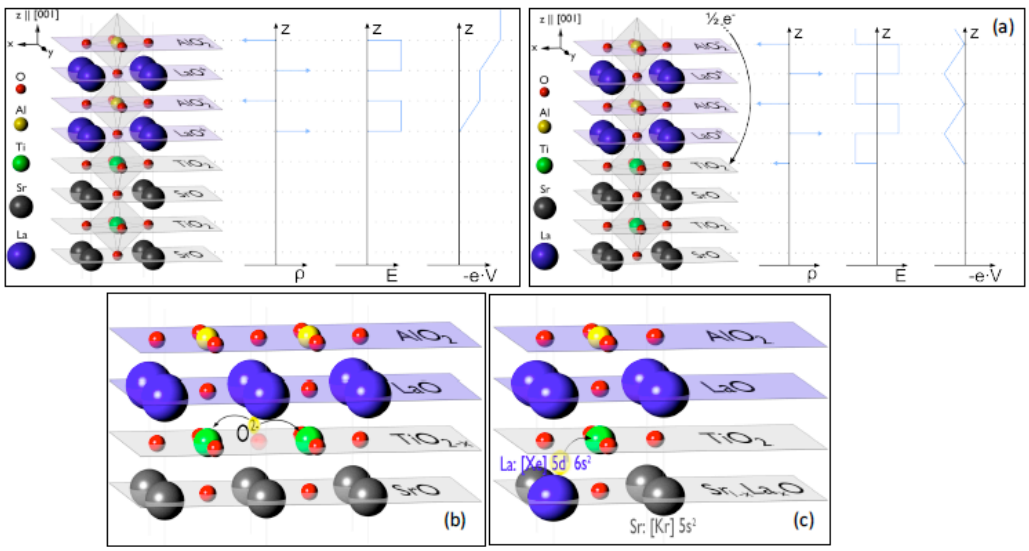

Fig. 2 (a) Top left pane: Heterostructures with TiO_2 terminated $SrTiO_3$ will lead to an increasing electrostatic energy of the electrons (-eV) when the thickness of $LaAlO_3$ is increased. The increase is a consequence of the internal electric field (E) coming from the excess charge (ρ) in each $LaAlO_3$ layer. To alleviate the electrostatic potential, electrons are internally transferred from the top $LaAlO_3$ layer to the interface titanium atoms whereby they are reduced to Ti^{3+}. This internal electron transfer then forms the interfacial electron gas. (b) Oxygen vacancies are considered as a possible mechanism for the formation of the electron gas. In the ionic $SrTiO_3$ lattice, oxygen is negatively charged. This excess charge is donated to the 3d-states of titanium when oxygen vacancies are created by removing neutral oxygen. (c) Lanthanum incorporation is considered a possible source of the electron gas. The presence of lanthanum incorporated into the $SrTiO_3$ near the interface will lead to an electronic doping

from the 5d electrons of lanthanum to the interfacial titanium atoms. Lanthanum can either be implanted into the substrate by plasma bombardment or inter-diffuse once present at the substrate surface.

As silicon is the basis of conventional electronics, STO is the foundation of oxide electronics. The results of recent years indicate that the surface of STO is where the future action takes place if silicon is to be replaced by oxide electronics. STO bulk properties have been studied for several decades in great detail [34]. However, until recently, studies on complex oxide heterostructures focused primarily on the electrical and magnetic properties of the conducting interface, avoiding the detailed influence of the STO substrate. The undoped STO at room temperature is a typical wide bandgap semiconductor, with an indirect bandgap of 3.2 eV and high dielectric constant (~ 370 -18000 for 296-1.4 K) [35]. Upon cooling, STO undergoes a second order structural phase transition at 105 K [36]. On approaching a lower temperature of 37 K, STO exhibits abnormalities in thermal conductivity, dielectricity, and ultrasonic attenuation, all of which are attributed to a transition to a quantum paraelectric state [37].

Motivated by the simple question of "why does every 2DEG discovered today involve an STO substrate?", we have recently found that chemical redox reactions at oxide interfaces can provide an alternative approach to understand the creation of a 2DEG [32]. This can alter the wideband insulator of stoichiometric STO into semiconducting, metallic, superconducting, or even magnetic states, depending on the concentration of oxygen vacancies. However, confining and controlling oxygen vacancies at the oxide interface are challenging issues. Our most recent results show that it is possible to realize such a confinement of oxygen vacancies in the proximity of the interface by growing epitaxially an ultrathin 2 nm insulating γ-Al_2O_3 film on STO. Remarkably, this new 2DEG shows record high electron mobility greater than 140,000 $cm^2V^{-1}s^{-1}$ at 2 K [38], which is 100 times larger than those obtained by other groups. These findings represent a significant step towards high-mobility oxide 2DEGs and necessarily force the oxide community to reconsider the mechanisms of complex oxide 2DEGs. By offering tremendous flexibility, such interfaces create emerging possibilities in designing new electronic systems. The design of high mobile samples achieved recently offers a unique opportunity to expand our understanding to the mechanism, which define why certain samples are "high mobile samples" and others are not. We have recently showed that it is possible to enhance the interfacial mobility via the following roots:

1. *Redox reactions* [32]. Chemical redox reactions at the oxide interface provide a way to create conduction. Regardless of the interface polarity, when depositing certain insulating oxides with higher oxygen affinity on the STO single crystalline substrate, the top layer can absorb oxygen from STO. Such an interfacial

chemical redox reaction results in a metallic interface between the amorphous LAO (a-LAO) film and the crystalline STO substrate, a-LAO/STO, the properties of which turn out to be quite similar to those of its all-crystalline counterpart. In these samples we have observed that carrier "freeze-out" at about 105K associated with low mobility of ~1000 cm^2/Vs at 2K corresponds to all-crystalline LAO/STO. At 105K the carrier density undergoes a sharp decrease (known as carrier "freeze-out") often associated with the cubic–tetragonal structural transition of STO. The band diagram of the STO/a-LAO system is given in Fig. 3a.

2. *Interface confined redox reactions* [38]. Since high quality epitaxial oxide heterostructures are normally formed at high temperatures, such as at 873K. At such a high temperature, oxygen diffuses over many micrometers in minutes since STO is a mixed conductor at high temperatures. This would completely level out any nanometer-scale steps in the oxygen concentration profiles of the STO-based heterostructures. In this vein, spatially confined redox reactions at the oxide interfaces turn out to be a central way to realize high mobility 2DEGs. Recently, we realized such interface confined oxygen vacancies at an epitaxial spinel-perovskite interface between γ-Al_2O_3 (GAO) and STO. Remarkably, this new type of oxide 2DEG shows an electron mobility record greater than 140,000 cm^2/Vs at 2 K, 100 times higher than that typically obtained in the perovskite-type oxide interfaces studied so far. In these interfaces we have observed no carrier "freeze-out" and the carrier density remains constant down to 2 K.
3. *Strain induced polarization* [39]. Recently, we have discovered a 2DEG at a nonpolar perovskite-type interface of $CaZrO_3$/STO with high electron mobility exceeding 60000 cm^2/Vs at 2 K. The sheet carrier density of the 2DEG exhibits critical thickness of t_c = 6 u.c. (~2.4 nm) for the occurrence of interface conduction which is slightly higher than that of the LAO/STO interface ($t_c \approx$ 1.6 nm). The band diagram of the CZO/STO system is given in Fig. 3b. The observation suggests that the polarization induced electronic reconstruction dominates the interface conduction. However, in distinct contrast to the LAO/STO system, where the carrier density normally exhibits a carrier freezing out behaviour at T = 105 K, the CZO/STO system exhibits an almost constant carrier density as a function of temperature, similar to the high mobility GAO/STO interface.
4. *Modulation doping* [40]. We have recently inserted a single unit cell-insulating layer of polar $La_{1-x}Sr_xMnO_3$ (x = 0, 1/8, and 1/3) at the interface between disordered $LaAlO_3$ and crystalline STO created at room temperature. We found that the electron mobility of the interfacial 2DEG exceeds 70000 cm^2/Vs at 2 K. The

LSMO buffer layer results in modulation doping in buffered d-LAO/STO and a milestone for future oxide electronics (will be discussed in more detailed below). For these interfaces we have observed no carrier freeze-out and this is also associated with high mobility samples. The band diagram of the STO/GAO system is shown in Fig. 3c.

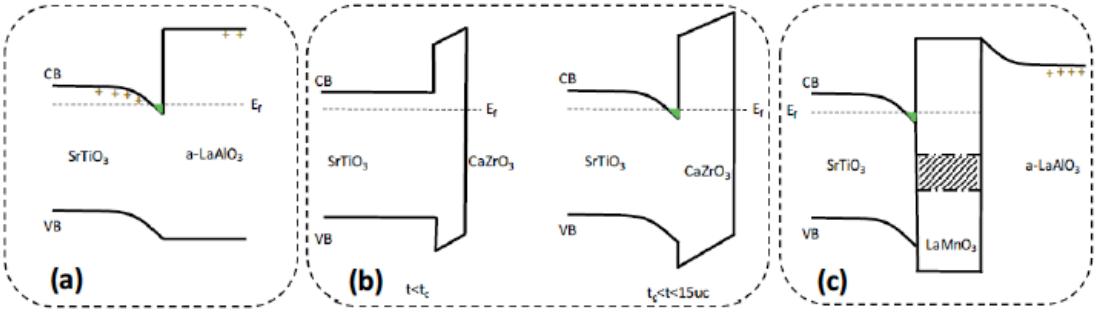

Fig. 3 Schematic band diagram of (a) STO-a-LAO, the (+) represents the position of the oxygen vacancies which donate the electrons to the interface, (b) STO/CZO system is characterised by critical thickness t_c in which above the interface becomes conductive and (c) STO/LMO/a-LAO, again the LMO spacer layer separate the positive donor ions (+) from the electrons.

Applications

The study of oxide 2DEGs is still at its very early age and the key question is if we can achieve parallel outstanding success for oxide interfaces similar to what we have experienced for the conventional Si-based analogues? High-mobility, two-dimensional electron systems are readily produced using "conventional" semiconductor heterostructures, and have led to fundamental breakthroughs in the study of quantum effects. Oxide systems are likewise interesting in that they hold the promise of novel phenomena due to the unique nature of the electronic states involved. Recently, it was shown that monolithically-integrated logic circuits utilizing the two-dimensional electron gas was fabricated [41]. This represents a milestone in the future use of these materials. To date, some the most interesting and intensely topics observed at these interfaces are: (1) Modulation doping – achieving high mobility samples, (2) the field effect, which is the ability to switch the resistance using externally applied electric fields, and (3) quantum effects in the transport coefficients.

Modulation-doping: The low-temperature electron mobility is a direct estimate of the mean free time and is commonly regarded as the 'figure of merit' for the characterization of 2DEG. It is determined easily by measuring the conductivity and the carrier density. The most important feature of a 2DEG is its high electron mobility, which is achieved using the so-called modulation-doping technique, which separates the positive donor ions from the electrons. Owing to the separation, electrons remain free and highly mobile. The spatial separation of the 2DEG from the donor impurity atoms is further increased by the introduction of a spacer

layer. The usage of the so-called modulation-doping technique has significantly increased the carrier mobility of 2DEGs in semiconductor heterostructures [42]. This led not only to the realization of high-electron-mobility field effect transistors (FET) but also to the discovery of the fractional quantum Hall effect in 2DEG samples of unprecedented structural perfection. We have recently inserted a single unit cell-insulating layer of polar $La_{1-x}Sr_xMnO_3$ (x = 0, 1/8, and 1/3) at the interface between disordered LAO and crystalline STO (see Fig. 4) created at room temperature [40]. We have found that the electron mobility of the interfacial 2DEG is enhanced by more than two orders of magnitude as compared to the case without a buffer layer. During the formation of 2DEG, electrons, which originate from positively ionized donors on the disordered LAO side, are firstly transferred to the spacer layer before filling the electronic shell of Ti ions on the STO side. The spacer layer act exactly as introduced in the modulation doped semiconductor heterostructures namely spatially separates the 2DEG electrons (on the STO side) and the ionized donors (on the disordered-LAO side). Our modulation-doped layer not only suppresses significantly the oxygen vacancies on the STO side but also results in modulation doping in buffered disordered-LAO/STO, which remains underexploited at complex oxide interfaces. Since most of complex oxide 2DEGs hold a similar electronic structure, the charge transfer induced modulation doping developed is expected to be a universal phenomenon.

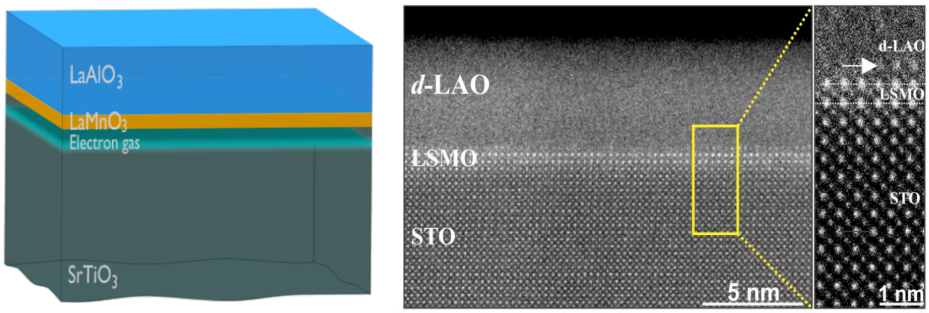

Fig. 4 To the left, a schematic illustration of the modulation doped sample (STO/LMO/a-LAO) and to the right HAADF-STEM images of the hetrostructure showing a single layer of LSMO [40]

Resistance switching: A particular interesting feature observed for crystalline-LAO/STO is the possibility of performing resistance switching upon application of an external electric field, which has led to the creation of numerous nano-electronic devices. At a LAO thickness of 3 u.c., the interfacial conductivity is showing insulating behaviour. Applying an external electric field will result, however, in a change in the interfacial conductivity analogue to the normal gated field effect transistor setup. It was demonstrated that resistance switching is realizable in LAO/STO heterostructures, by applying the electric field in two general setups: using a sample-wide back-gate [31] or using a conducting AFM (cAFM) tip [43]. For both setups the resistance switching is shown to be possible for heterostructures with 3 u.c. LAO, whereas 2 or

4 u.c. shows little or no switching [29,43]. Fig. 5 shows a schematic illustration of the principle of "writing" with cAFM conductive layer. The change in resistance show pronounced memory effect upon removal of the electric field with a remarkably high retention time. However, there is still no consensus for the mechanisms which play role in this metal-insulator-transition. Interestingly, there also seems to be experimental evidence supporting that the presence of water in the atmosphere can play a role in the ability to induce the resistance switching by cAFM [44]. It is demonstrated that in dry air or under a vacuum of 2.4 x 10^{-5} mbar the interface loses its ability to induce conductivity with cAFM, whereas introduction of ambient air results in successful resistance switching. This is suggested to be caused by water dissociating into the OH^- and H^+ on the surface of LAO. The concentrations of these charged species can then be modulated by the biased cAFM tip thereby leading to charge carriers at the interface. Strikingly, this is in contrast to the back-gate induced resistance switching, where no effect of vacuum is observed [31].

As for the switching with the back-gate, it seems however that by simple electrostatic energy considerations it is unlikely that any direct structural changes can be feasible by applying an external field using a back-gate relative far from the interface. It is therefore an open question whether the origin in the case of back-gate induced resistance switching is purely electronic or not. As for the mechanism, which exists in the cAFM experiments, it is initially proposed that the resistance switching is a result of the charged tip repelling oxygen ions thereby creating a path of oxygen vacancies at the surface, where the tip has been scanning [43]. This locally elevated vacancy concentration is thought to result in local doping of the interface. Upon assuming that the vacancies are little mobile by themselves at room temperature, this structural modulation is thereby consistent with the very long decay time to the insulating state. Recently, we have discovered a non-volatile, bipolar resistive switching in the oxide heterostructure composed of a STO single crystal on which a thin film of a-LAO is deposited [45]. The change in the sheet resistance exceeds 3 orders of magnitude at room temperature and was accompanied with a large modulation of the charge carriers. The microscopic origin of the change in the resistivity is discussed and explained by either

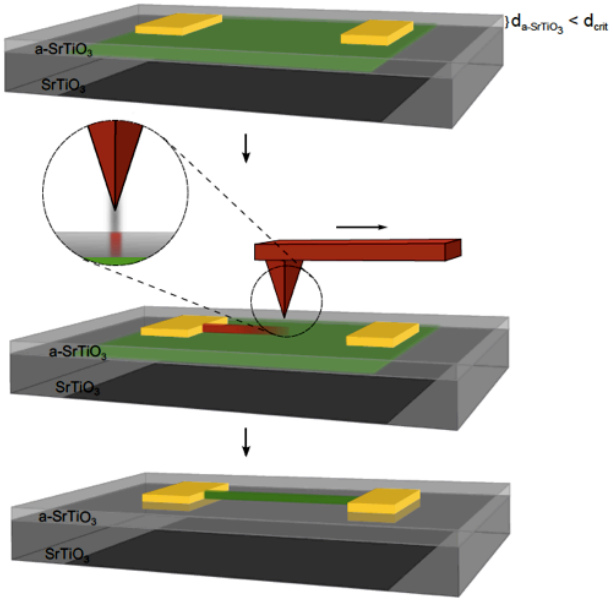

Fig. 5 Schematic illustration of the principle of writing conductive lines with cAFM.

electro-migration of oxygen vacancies or the presence of charge trapping states [45,46]. Furthermore, we have also recently being able to control the carrier density by shining light using the photoconductivity effect in addition to the back-gate [30]. We found that light illumination decreases, rather than increases, the carrier density of the gas when the interface is negatively gated through the STO layer, and the density drop can be 20 times as large as that caused by the conventional capacitive effect. These findings open the possibility of employing these effects to module the carriers at the interface.

Quantum Hall effect: Controlling electronic confinement in the solid state is increasingly challenging as the dimensionality and size scale are reduced. This can lead to new physics in oxide mesoscopic devices. Beyond Quantum Hall Effect (QHE), many unexpected results are expected in these complex mesoscopic oxide devices, fabrication of which has become possible recently, with the typical size in the range of 100 nm. Recent technical advances in the atomic-scale growth of oxide thin films have resulted in the creation of high-mobility 2DEG at heterointerfaces based on either ZnO [47] or STO [38,39,40]. Remarkably, the mobility enhancement made in polar MgZnO/ZnO heterostructures has for the first time led to the observation of both integer and fractional quantum Hall effect in all-oxide devices [48]. The conducting states of ZnO-based heterostructures are, however, similar to the conventional semiconductor heterostructures, derived from *sp* hybrid orbitals with a largely covalent nature. In contrast, the interface conduction in STO-based heterostructures originates from slightly overlapping Ti 3d-orbitals [49], where the resulting ionic bonds lead to a strong coupling between the lattice, charge and spin degrees of freedom. Fig. 6 shows a schematic illustration of the conduction edges at the interface, *i.e.* the electrical current is carried by electrons with their orbit centre close to the edge known as "skipping orbitals". We have recently observed the Quantum Hall Effect (QHE) at a modulation-doped oxide interface where the observed quantization is consistent with an interface system comprised of multiple coupled quantum wells [50]. Multiple quantum wells have already been predicted theoretically for the crystalline LAO/STO interface [51]. However, so far they have not been experimentally verified. Is the appearance of multiple quantum wells universal for all STO based heterostructures? Our understanding of the origin of the charge and its confinement will deepen our understanding of the nature of the conducting interface and the

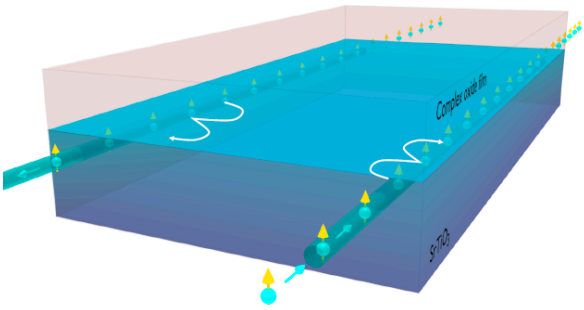

Fig. 6 A schematic illustration of the conducting edge states at the interface in which electrons bending to opposite directions with what is known as skipping orbital motions.

enhancement of the mobility and will open the door for new and unseen quantum phenomena in these samples.

Outlook

One of the long-standing questions is how the transport properties at the interfaces related to the structural transition that the STO undergoes, i.e. from cubic to tetragonal at around 105 K. For the LAO/STO it was previously found that the current flow in conductive narrow paths oriented along the crystallographic axes, embedded in a less conductive background [52, 53]. The configuration of these paths changed on thermal cycling above the STO cubic-to-tetragonal structural transition temperature, implying that the local conductivity is strongly modified by the STO tetragonal domain structure. However, is this behaviour is true only for this system or it is universal to all STO based hetrostructures? What is the role of the top layer on the transition? Can we control the domain-structure and how it influences the carrier density or/and mobility? A large carrier "freeze-out" towards low temperatures was previously observed in the cases of $LaAlO_3$/STO [54], $LaTiO_3$/STO [55], $LaGaO_3$/STO [56] and $CaHfO_3$/STO [57] which is also associated with low mobility of approximately 1000 cm^2/Vs at 2 K. Unlike what is observed in these samples, LAO/STO with capping layer of $SrCuO_2$ [58] shows no "freeze-out" with high mobility of approximately 50000 cm^2/Vs at 2 K, in our recent observation of the high mobile samples, GAO/ STO [38], $CaZrO_3$/STO [39] and the buffered disordered-LAO/STO [40] the carrier density remains constant at all temperatures measured, implying the absence of carrier "freeze-out" and showing high carrier mobility 60000-140000 cm^2/Vs at 2 K. Is this something related intrinsically to the STO or does it relate to the "cleanliness" of the interface? The full understanding of such properties remains to be established.

2. Interface effects in Oxygen Ionic conductors and complex heterostructures

Ionic conductors are an important class of materials which find applications in several key-technologies, *e.g.* for energy conversion and storage. Among the various ionic conductors the oxygen ions conductors, *i.e.* conductors of oxygen ionic vacancies, such as ZrO_2, CeO_2, Bi_2O_3, $LaMnO_3$, $La(Co,Fe)O_3$, *etc*. are the basic compounds for the state of the art solid oxide fuel cell, oxygen gas separation membranes, catalysis, sensors [59-68]. Such materials have been also recently proposed for new interesting applications in novel solid state memory devices [69,70].

In ionic conductors, the charges are structural and electronic defects highly localized at the ionic lattice. In oxygen conductors, the charges are "intrinsic" oxygen vacancies and electronic defects (electrons and holes) are naturally formed at the lattice as thermal defects. A typical example is the reduction reaction in metal oxides (*MeO*), written in Kröger-Vink notation, as:

$$O_o \rightarrow V_O^{\cdot\cdot} + 2e' + \tfrac{1}{2} O_2\,(g),$$

where structural oxygen (O_o) is lost as gas (O_2) and leaves double positive charge Schottky-like oxygen vacancies ($Vo^{\cdot\cdot}$) and n-type charge, i.e. electrons (e') at the cation sites.

In other cases, defects are formed by "extrinsic" factors, *e.g.* by doping the material with aliovalent cations. In this latter case, large amount of oxygen defects can be introduced using the acceptor dopant (e.g. A' acceptor carrying one electron) which substitutes the hosting cations (*Me*). The substitution by acceptor dopant A' at the *Me* site leads to oxygen vacancies formation as:

$$2A'_{Me} \rightarrow V^{\cdot\cdot}_O + \tfrac{1}{2}\, O_2$$

Conversely, introducing donor dopant ($D^{\cdot}$) reduces the number of oxygen defect and increase the population of electronic holes in the structure. Mixed ionic and electronic conductors (MIECs) arise in ionics material by simultaneous formation of oxygen defects and electronic defect which are changes of cations valence in the lattice, *i.e.* donor and acceptor sites. Yet, the latter can both introduce electronic, positive ($h^{\cdot}$, by donor doping) and negative (e', by acceptor doping) defects. Such electronic defects are also known as polarons. In ionic compounds, all the possible defects have to be electrically balanced leading to neutrally charged compound [60]. The electrical conductivity of ionic compounds is based on formation and mobility of punctual defects under bias of electrical field. The formation of defects in materials is related to thermodynamical factors and by mass action relation, which includes the conservation of the mass also at the solid-oxygen gas equilibrium [60].

As for the mobility, due to the ionic bonding of these materials, the charges are generally electrostatically bounded to the lattice and a certain thermal energy (typically between 0.3-2 eV) is required to activate their migration. In a simplified model often used to describe the charge migration in ionics, electrical charges such as oxygen defects and/or polarons "jump" by thermally activated hopping mechanisms from a position to another equivalent site in the lattice. This occurs under the driving force of applied electrical and/or electrochemical fields [71].

MeO Interfaces

Defects are responsible for the electrical properties of ionic metal oxides. However, crystalline lattice is in reality largely defective with punctual but also with extended defects. Presence of two dimensional hetero-phase interfaces and /or other forms of lattice discontinuities such as linear dislocation, large punctual vacancies associations *etc.*, can introduce "perturbation" in the ionic lattice and greatly affect the charge transport mechanisms [72]. Among all the possible extended defects, 2D interfaces are the most important and technologically relevant. Interfaces in oxygen ionic oxide are generally more defective and energetic than the bulk [73]. For some ionic conductors such conditions can trigger enhanced charge transport phenomena as result of both defect formation and fast charge mobility which occur at lower energies than for the lattice at the bulk [61-63, 73-75]. In the case of oxygen ionic conductors, however, conduction mechanisms at the interfaces are complicated by the nature of the oxygen vacancies, which are substitutional Schottky-like defects, as well as by the chemistry of the materials, where dopants and other elements easily segregate at the interface imposing local "extrinsic" factors to the conduction mechanisms. These important factors are widely proved in the case of solid-gas interfaces (not treated here), where structural strain, high vacancies concentration and elemental segregation can, *e.g.*, greatly affect catalytic performances of the materials by changing gas sorption-desorption and surface diffusion mechanisms [76-78]. On the other hand, solid-solid interfaces can present a wide range of features and properties and in some cases these factors can result beneficial for applications as in thin film-based ionic devices [79]. Since defects concentration and their mobility are the parameters influencing the conductivity, we consider here the degree of disorder at the interface as the key factor in varying the electrical properties. Some examples of solid-solid interfaces, which are relevant for the discussion, are also schematically summarized in Fig. 7. Particularly, Fig. 7a and 7b show two examples of highly defective and disordered interfaces. These are especially the cases of naturally formed interfaces in polycrystalline materials and non-epitaxial films [79], where two adjacent structures are discontinuous and the boundary thus highly disordered. On the other hand, Figure 7c shows a schematic representation of an "ordered" interface. This is commonly formed by epitaxial growth, *e.g.* in thin films deposition, where coherent lattice

with same crystallographic orientation is maintained from a material to another giving a more or less distorted interface. In this latter case the degree of disorder depends on the crystalline mismatch between the pristine components. Other semi-coherent cases which are combinations of these cases are also possible and are also briefly discussed here.

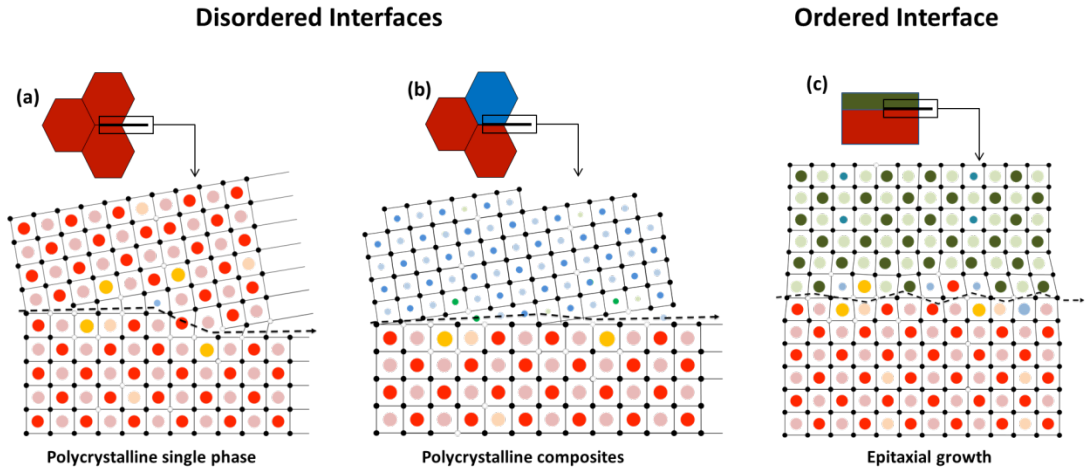

Fig. 7 Typical cases of solid-solid interfaces in metal oxides: disordered interfaces in polycrystalline (a), composite materials (b) and ordered hetero-phase interface in epitaxial films (c).

"Disordered interfaces"

The effect on charge migration process at "naturally" disordered interfaces, such as the grain boundary of polycrystalline (Fig. 7a) system and interphase in composites (Fig. 7b), is an important topic which has been studied since the early seventies and formalized in the so called "brick model" and "space-charge layer" model [72, 80-82]. A phenomenon that can be distinguished is the transport across and along disordered interfaces. Across the interface, disorder between two crystalline domains (*e.g.* grain-grain interface, as in Fig. 7a) or lattice mismatching (*e.g.* phase-phase interface, as in Fig. 7b) usually cause blocking effects for the oxygen vacancies migration mechanisms resulting a decrease in ionic conductivity [72]. This is attributed to the excess of charges at the disordered interface core which creates high electrostatic potential at the interface, attracting and thus "blocking" the charge migration. Along the interfaces, enhanced ionic conduction has been observed in some solid state ionics. According to the brick-model, ionic transport across interface is dominant in large polycrystalline systems while effects along interfaces become dominant, and measurable, in the so called "nanoionics", where the interface becomes prevalent with respect of the bulk [61-63, 73-75]. Another characteristic is the nature of the ionic conductivity. Several experimental evidences show that disordered interfaces in crystalline materials can induce fast ionic conductivity, even in proximity of room temperature [73, 74, 83]. This mainly observed in some ion conductors, called superionics, such as αAgI, Ag-/Li-based oxides, sulphide glasses, β-Al_2O_3. [74, 83]. For these materials the high level of ionic conductivity is due to the

notably reduction of defect formation and especially due to the reduction of migration energies at the disordered regions. This is especially the case for interstitial charges (*e.g.* Frenkel defects) which show, at the disordered interface, low energy migration paths between sites with similar energies [83]. For oxygen ion conductors, the conduction mechanisms are further complicated by the dual nature of the oxygen ions, which is a result of the Schottky-defects that play role both as bonding and defective charge carrier. Several studies report that for oxygen ionics, disorder of the lattice at the interface can lead to enhanced conductivity at disordered interfaces as the net effect of several factors which strictly depend on the chemical nature of the lattice [73, 84]. Particularly, disordered interfaces can easily undergo simultaneous charges accumulations, depletion or inversion, due to spontaneous effect of oxygen defect formation and cation trapping (*e.g.* impurities segregation) at the disordered lattice [73]. These factors usually lead to remarkable formation of electronic defects, which overlapped the existing ionic conductivity, increase the total conduction even in dominantly ionically conducting or dielectric materials. Effects of interfacial conductivity enhancement in a few orders of magnitude due to electronic contribution were thus observed in nanometric polycrystalline metals oxides such as Y-doped ZrO_2, CeO_2 [61, 73], Fe-doped $SrTiO_3$ [85], NiO, ZnO, Al_2O_3, MgO [86-89]. Similar effects are registered also in hetero-interfaces (as in Fig. 7b) containing nano-composite of ionic materials and in ionics mixed with insulating materials, indicating that the interface is the dominant factor [89]. A simple explanation for these phenomena lays in the fact that ionic compounds must be electrostatically neutral, *i.e.* the accumulation of charges (*e.g.* positively charged oxygen vacancies) at the disordered regions necessarily leads to a redistribution of electronic carriers (*e.g.* negatively charged e´ defects) at the interface. Interestingly, in oxygen ionics such charging effects occur not only at the disordered core of the interface but also at the bulk-like lattice layer, or region, which is adjacent to the highly disordered interfacial core. The conductive process at these interfaces has been especially studied for polycrystalline systems and it is formalized in the so-called "space charge layer" (SCL) model [90]. This indicates that defects formation and accumulation at the disordered interface induce concentration profiles of opposite charges in the regions adjacent to the disordered region. According to the model, opposite charges accumulation and depletion occur to balance the core and the interfacial region including such charges profiles and is called space charge layer (SCL). Fig. 8 illustrates schematically the SCL model proposed for oxygen ions metal oxides [73, 90]. In analogy with the Schottky-barrier model used for semiconductors and liquid electrolytes, the SCL thickness depends on the chemical nature and dielectric properties of the interface. The extension of the charging at the SCL is defined by the Debye length. This represents the geometrical "thickness" of the charged-layer which is contributing to the conductive process at the interface. At the simplest level of the analysis, the Debye length is expressed by the Debye–Hückel formulation [91]:

$$\lambda_D = (\varepsilon_r \varepsilon_0 \varepsilon_B T / \sum_{i=1}^{N} q_i^2 n_i)^2 \qquad (1)$$

This equation is generically used to describe the SCL in materials with N different species of charges, the *i-th* species carries with charge, q_i, and concentrations, n_i. According to this model, the charging arises naturally and can be described by the thermodynamic factors of the defective lattice when the charges are distributed in a medium characterized only by its relative permittivity, ε [91]. This model is therefore based on the simplification that Debye length depends on the defect concentration at the bulk and not on the electrostatic field due to the accumulated defect at the interface, $\Delta\phi(x)$, where x is the distance from the interface core [73]. The equation indicates also that the overall charged species contribute to the SCL in the same way, regardless of the sign of their charges and the length which is pronounced at reduced temperature as well as in intrinsic conductors, where the bulk defect concentration is lower [61]. The SCL and charges are thus conveniently linked by the relation $\lambda_D \propto n^{-1/2}$, which, for a typical ionic conductor (*e.g.* YSZ) in the range of 700 K, gives values of tens of nanometers of the Debye length (λ_D) [61, 84]. The simplicity of the SCL approach, *i.e.* the actual extension and the charges profiles of the SCL and thus its contribution to the total conductivity, is affected by several additional factors. An important example was raised by Maier [73, 90] and Tschöpe [92] for nanometric CeO_{2-x} polycrystalline systems, where the interfacial conductivity is dominant over the total conductivity [73]. Interestingly, this case comprises the dopant and concentration (or impurities), showing that the width of the actual space charge zone (λ^*) is larger than λ_D and depends on the electrical potential at the core interface $\Delta\phi(0)$. This was expressed in the equation [90]:

$$\lambda^* = \lambda_D \left(\frac{4q}{k_B T} \Delta\phi(0)\right)^{0.5} \qquad (2)$$

This is in contrast to the calculation of λ_D which is exclusively determined by bulk parameter and it indicates that even in acceptor doped conditions (*i.e.* extrinsic conductors), for which λ_D is small, the actual SCL is wide where $\Delta\phi(0)$ is large, *e.g.* caused by the effect of the uncompensated charges segregated at the core interface. This was formalized in the Mott-Schottky type model, which assumes that the dopants are immobile while the counter majority of the charge carriers (*e.g.* $V_O^{\bullet\bullet}$) is depleted from the SCL. In such conditions the dopant profile is assumed constant and the conductivity along the interface is found [90]:

$$\sigma_{tot}^{''} = \lambda^{*}\left(\frac{4F\mu_i}{L}\right)\frac{n_{i(interface)}}{2\ln\left(\frac{n_{i(interface)}}{n_{i(bulk)}}\right)} \qquad (3)$$

where F is the faraday constant, μ_i is the individual charge mobility, L is the total thickness of the materials and n_i is the concentration of the different species. The charge profile calculated for $CeO_{2-\delta}$ is schematically illustrated in Fig. 8, where the positive carriers, *i.e.* $VO^{\bullet\bullet}$ (and $h^{\bullet}$), and negative charges (n-type polarons) are formed and accumulated at the SCL to compensate the highly oxygen defective interface core. In terms of electrical properties, assuming similar mobility for the different carriers, both ionic and electronic transport is mainly enhanced along the SCL parallel to the interfacial core regions because the core is extremely thin, jammed of defects and thus very resistive. As a net result, the space charge potential leads to oxygen vacancies depletion at the SCL which can severely hinders the ionic transport, dominating the conduction at the interface.

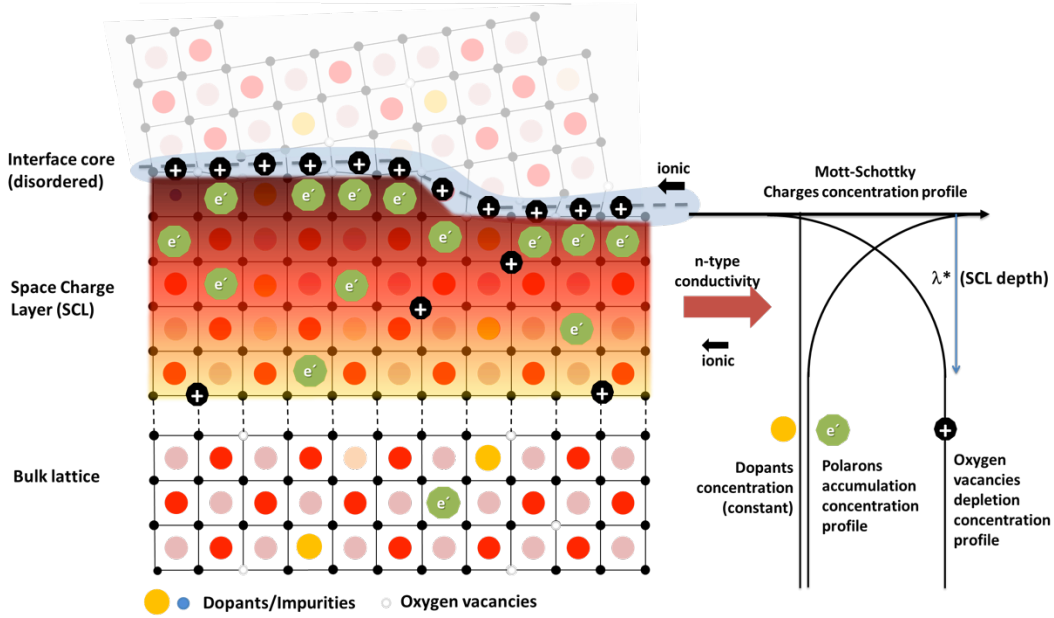

Fig. 8 Schematic representation of the SCL layer and related charge profile according to the Mott-Schottky model [73, 90, 92].

Due to complexity of the disordered interfaces, the proposed models fit well only a few experimental cases, *i.e.* especially metal oxides dominated by intrinsic ionic conductivity and large SCL [73]. For other extrinsic cases such as YSZ and ceria solid solutions the experimental evidences are less clear [61, 73, 84]. As discussed above, the thickness of the SCL can be reduced by the large concentration of charge carriers, dopants, aliovalent impurities and even the material preparation methods all of which have shown to affect further the profile of the charge carriers' concentration [61, 73, 85, 93-95]. Different profiles of charge concentration are therefore possible to implement and some alternative models

have been further considered [73, 90]. For these cases, other models such as the Gouy-Chapman [90] interface, where the dopant/impurity profile change as function of the distance from the interface, have also been proposed for disordered interfaces with inhomogeneous dopant profile. However, no experimental evidences have been proven this approach so far. Other cases of very large disorder interface and thin bulk (*e.g.* in ultra-thin films) enter in the sub-Debye range of highly disordered interface is almost an unexplored matter [73]. Conductivity at the disordered core is difficult to estimate because of the accumulation of several effects such as lattice strain, phase changes, dislocations and vacancies association. In the SCL-core boundary, other more obscure factors can take place. These can be the confinement and interaction effects of electrons and ions such as associations, but also segregated dopant and impurities, strain effects, *etc*. The strain becomes an important factor also in nanocrystalline thin films, where effect of disordered interfaces overlaps with the strain at the lattice which may be due to the mechanical constrain at the substrate and/or by the residual stress created at the deposition stage. These factors are often not negligible, leading to a large variety different of electrical behaviours [79].

Despite the variety of potential factors affecting the conductivity, the most probable effect observed at the disordered interfaces is the SCL formation. As result, the overall conductivity of interfacial region increases and the activation energy for the charge migration decreases. However, this can be due to the increase of mixed carriers' population, *e.g.* rise of e´ defects with dominant n-type conductivity, rather than an increase of oxygen ionic conductivity [92]. As discussed above, this can overlap or even bypass the bulk transport, controlling the overall conductivity in oxygen ionic conductors. Fast oxygen vacancies at the interfaces are indeed very desirable because it would allow decreasing ohmic losses but the presence of electronic leak at these materials is detrimental. Therefore, increasing the oxygen ionic conductivity selectively in disordered interfaces by creating fast conduction paths is somehow questionable.

Coherent and semi-coherent interfaces

Disordered interfaces are formed naturally at the ionic compounds and can easily result in uncontrolled defective concentration, composition and thus variety of electrical properties. On the other hand, coherent ordered interfaces can be finely tuned in epitaxial thin film, heterostructures and multilayers systems [63]. These interfaces in metal oxides have a growing technological relevance and can be fabricated by a large variety of deposition methods [96]. As schematically illustrated in Fig. 7c, crystalline order is kept at the hetero-phase interface by matching similar lattices or by matching different crystals which present orientations with similar atomic distances [96]. The lattices differences of the two phases result in slight distortions and/or occasional defects which are mostly localized at the interface and involve few atomic layers [97]. Some examples of such defects resulting in crystalline disorder are

linear dislocations, vacancies-dopant associates and especially lattice strain resulting from *atomic peening*, which occurs to reduce the interfacial energy during the deposition [98]. In thin films deposition, in the case of large mismatch between the substrate and the film, the occurrence of dislocations starts soon after film formation to accommodate the large mismatch with typically large mosaic spread accompanied by columnar growth. The tremendous sensitivity of oxides properties to strain and localized defects at interfaces is widely reported and is influence *e.g.* the magnetic and transport properties [99]. For electronic materials such as semiconductors, high temperature superconductors, diluted magnetic semiconductors, the presence of distorted coherent interfaces and localized defects result in significant and quantifiable effects on charge-carrier density and mobility (see the first part of this review paper). For ionic compounds, such as CaF_2-BaF_2 heterostructures, tuned interfaces at multilayers are of great enhancement of the ionic transport, *e.g.* F^- ions [63]. Tuning of these factors is demonstrated to be a powerful method of modifying materials properties. On the other hand, despite the fact that the effect of strain on oxygen ions conductivity is attracting notable interest, experimental evidenced are still needed and some of the results are controversial [100].

Effect of strain

For highly coherent interfaces, the dominant factor is the *lattice strain* imposed by the growth of a second lattice on a dissimilar substrate lattice, *i.e.* strain at the hetero-phase boundary. The biaxial strain parallel at the interface plane, ε_{xy}, where conversely ε_z refers to the out-of-plane direction, is generally calculated as the difference between the lattices with respect to the substrate lattice. The lattice mismatch, *f*, of the matching interatomic distances d_{khl}, is simply calculated by the following simple equation:

$$f = \frac{d^B_{khl} - d^A_{khl}}{d^A_{khl}} \approx \varepsilon_{xy} \qquad (4)$$

The mismatch between two coherent metal oxides is usually small, often below 5-6 % and it nearly corresponds to the ε_{xy} in the materials at the interface [101]. In a rather simplified fashion, however, the lattice mismatch and the corresponding strain are considered as "static" parameters: *f* is calculated on the theoretical lattices at room temperature. This assumption does not consider that "dynamical" factors can be in play in the actual interface strain. Some of such factors are:

- The substrate surface may undergo distortion before the deposition and thus *f* is not representative of the actual strain at the interface.

- Materials have usually different thermal expansion and the strain changes with temperature
- As formulated in equation (4) the strain refers to the pure elastic domain, where the lattice does not undergo "plastic" deformation and it maintains its symmetry. However, rearrangement of the lattice and relaxation are indeed possible at the interface by punctual and extensive defects formations, phase transitions, chemical interactions and element interdiffusion. All these factors can occur, especially at high temperatures, where ionic conductivity is generally measured.

As an example of the latter case, it is known that Young´s modulus in YSZ is a function of temperature due to the punctual defects formation [102]. From a phenomenological point of view, the effect of strain on conductivity often refers to thin films with different thickness, where the influence of the elastic lattice strain is expected to be very limited. Calculations show that for metal oxides such as CeO_2 and ZrO, MgO, Al_2O_3, STO *etc*., the effect of elastic strain decays exponentially in the out-of-plane direction films and for films above 100-200 nm lattice strain is not anymore dominated [101]. On the other hand, as the films get thinner, the film-substrate interface interaction becomes more significant and the influence of the Debye length on the disordered lattice increases [101].

The great interested in the lattice strain raises from a few experimental evidences of fast conductivity in metal oxides. In one case, it was reported a 7 orders of ionic conductivity enhancement in YSZ and it has been widely proved to be induced by combination of electronic and ionic conductivity [103]. On the other hand, theoretical calculation and simulations suggest that interfacial tensile strain is beneficial and can improve the oxygen ionic conductivity through changes in the hopping sites and frequencies, due to a substantial variation of the enthalpies of oxygen-vacancy migration and association [104]. The key factors for enabling fast oxygen transport in strained lattice have been thus discussed in a growing number of publications describing the combined *electro-chemo-mechanic* effects on oxygen ion conductivity both on biaxial and isotropic strain [104, 105]. Particularly, Sousa *et al.* have employed static lattice simulations to examine the effect of isotropic and biaxial strain on the migration thermodynamics of oxygen vacancies in fluorite-structured ceria. These findings indicate that strain can considerably alter the migration thermodynamics, enhancing extrinsic ionic conductivity by a few orders of magnitude [106]. Using a model based on the elastic properties of YSZ, Schichtel *et al.* estimated an increase of 2.5 orders of magnitude in the ionic conductivity of YSZ at 7% isotropic tensile strain [107]. By Monte Carlo-based calculations on YSZ, Kushima and Yildiz [108] identified competing processes acting on oxygen diffusivity upon applied strain: for low isotropic tensile strain (up to 4%), oxygen diffusion can increase by 3.8 orders of magnitude at low temperatures due to the fact that the

migration barrier is reduced by 0.4 eV. While, for strain higher than critical values (6-8%) the break and re-form of oxygen bonds can decrease the diffusivity as a result of plastic relaxation leading to lattice disorder increasing the migration barriers. For the compressive strain, Hirschfeld and Lustfeld used DFT with the Nudged Elastic Band (NEB) calculations applied on migration barrier for oxygen ions in zirconia and showed that the migration energy increases under compression to a maximum value and than decrease under expansion [109]. On the other hand, potential strain conditions under which the migration barrier strongly decreases were also identified and simulated for fast anisotropic oxygen diffusion in YSZ [110].

Other theoretical studies and reviews reports the combined theoretical calculations and experimental observations of induced plastic strain at the film introducing disordered characteristics such as grain boundaries, defect-dopant/impurities associate, dislocations. A*b initio* calculations on Y-doped $CeO_{2-\delta}$ lattice, by Burbano *et al.*, show that for a modest enhancement of the conductivity in isotropically strained bulk results in a lower bi-axially strained thin film with disordered atomic configuration [111]. Korte *et al.* [101] analysed the influence of elastic strain in columnar thin films by analytical model based on biaxial mechanical strain caused by lattice mismatch and elastic deformation along the columnar grain boundaries. The analysis was carried out by considering a variety of experimental results and concludes that changes in interface transport are mainly occurring in extrinsic ionic conductors which caused by strain as well as by the formations of misfit dislocations or disordered transition regions [101]. However, the picture becomes more complex when dopants, anisotropic strain and lattice disorder effect overlap. The role of materials' interfaces/grain boundaries on the anion conductivity using static atomistic simulations on ZrO_2 /CeO_2 and ThO_2 /CeO_2 interfaces was conducted by Aidh *et al.* [112], showing key interface issues of oxygen vacancy migration barriers at interfaces in the absence and presence of dopants, and oxygen vacancy-dopant binding energies at interfaces. The simulations suggest that the concept of strained prevails in the absence of segregated dopants [112]. Shi *et al.* [104] have recently discussed the thermodynamical factors, which can have an impact on the conductivity of nano-crystalline Gd-doped ceria (CGO, $Ce_{0.8}Gd_{0.2}O_{1.9-\delta}$), in light of experimental results on self-standing and supported nanocrystalline thin films, showing a clear correlation between compressive strain (*ca.* 2.7%) and increase or oxygen activation energy (+ 0.27 eV). In another recent paper, Sun *et al.* simulated the effect of dislocation in bulk doped ceria, concluding that dislocations can bring vacancies associative effects around the dislocation which slow down the ion transport [113].

On the phenomenological results, the large variety of microstructures, substrates and thicknesses of the films and heterostructure make a clear analysis very difficult and often contradictory. Therefore, a typical simple example such as epitaxial YSZ film can result in a

variety of electrical properties, varying in more than 3 orders of magnitude in conductivity depending on the substrate, presence of dislocations, elastic strain in thin film or heterostructure configuration [101]. Only a very few reports consider the pure strain case, free of the "plastic" effect of disordered region such as dislocations or grain boundaries. Li *et al.* [114] have studied YSZ comparing highly coherent YSZ/$Gd_2Zr_2O_7$ with YSZ/CeO_2 heterostructures where dislocations are present. The study suggested that the relaxation of elastic strain brought by dislocations does not enhance ionic conductivity [114]. This is however in contrast with Sillassen *et al.* [116] on semi-coherent 58 nm thick epitaxial columnar YSZ films on MgO which shows 3.5 orders of magnitude enhancement in ionic conductivities, which, on the other hand, agrees with the quantitative predictions of Kushima and Yildiz [108, 115, 116]. For this experimental case, Sillassen *et al.* [116] proposed a superposition of two parallel contributions - one is due to the bulk and the other was attributed to the film-substrate interface, indicating a transition temperature of 350 °C, where low energy contribution from the interface is dominating over the "bulk-like" YSZ conductivity. However, it is still not clear whether dislocations and other form of disorder defects can affect the ionic conductivity by space charge region effects [116].

In our previous work, we proposed comparative and systematic approach for pure strained interfaces in highly doped CeO_2 and YSZ. In Kant *et al.*, we used highly coherent CGO thin films of 250 nm on buffered MgO(001)/STO substrates to evaluate the effect of strain in highly coherent interface using several thicknesses at STO buffer (10, 20 and 50 nm) [117, 118]. Fig. 9 shows schematically how modulating the thickness of the buffer layer is used to tune the strain at the STO/CGO interface.

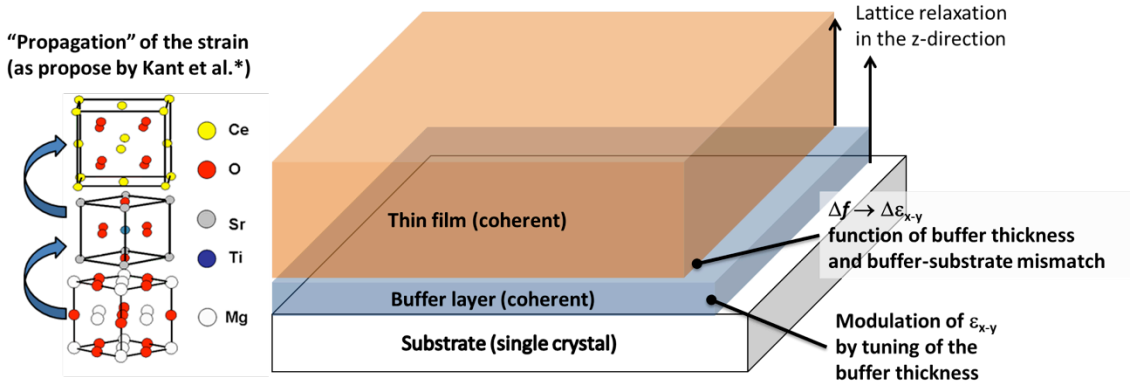

Fig. 9 Schematic representation of the buffer concept used to preserve the epitaxial coherency at the thin film and tune the interface strain *[59, 60].

The use of the STO buffer layers at the MgO(001) substrate allows preserving the structural coherency throughout the structure due to the low mismatch $f_{MgO/STO} < 1.1\%$. On the other hand, the different thicknesses of the STO(001) create a differential strain effect at the STO

lattice, which decreases with increasing the thickness and can be "propagated" to the CGO thin films creating a tailored mismatch $\Delta f_{STO/CGO}$ from 0.6 to 1.9 %. While the bulky nature of the CGO film (250 nm) allowed excluding any SCL effects or contribution form the STO buffer, the transport measurements indicated that CGO thin films enhances the *in-plane* ionic conductivity in the films of *ca.* one order of magnitude due to buffer layer induced by a strain of *ca.* 2%. As proposed by Maier for CaF_2/BaF_2 heterostructure, the key parameter for increasing the ionic conductivity at the interfaces lies in the confinement of nano and atomic scale heterostructures by tuning the lattice strain between the layers and tuning the number of the interfaces [63]. In Sanna *et al.*, we thus proposed a fine tuning of strain in highly coherent Sm doped Ceria (SDC)/YSZ heterostructure: a) by using STO buffer layer on MgO substrates to preserve the lattice coherency in the deposition [119], and b) by varying thickness and number of layers at the SDC/YSZ multilayer to propagate the strain at the interfaces [120]. The case showed a moderate effect of tensile strain of the interface in extrinsic conductor for thin films with an enhancement of oxygen ionic conductivity below 2 orders of magnitude. The experiments also showed limited electronic contribution in thin film below 5 nm, implying that forming coherent hetero interfaces with controlled lattice strain and dominant ionic contribution is indeed feasible for thin film below the Debye length if highly coherent [119, 120]. In a more recent paper, Kort *et al.* used multilayer of YSZ with dielectric Me_2O_3 phases (i.e. YSZ/Me_2O_3, Me = Y, Sc, Lu) columnar heterostructure to tune the strain from compressive (Lu_2O_3) to tensile (Sc_2O_3 and Y_2O_3), showing similar results [101, 121]. In this case, however, the presence grain boundary at the film opens the question about the effect of local strain relaxation or the presence of SCL. This is especially important due to the fact that high phase boundary in disordered CeO_2/YSZ heterostructures showed no conductivity effects despite high nominal tensile strain of up to 5.2% [122]. For the compressive strain, Schweiger *et al.* used a micro-electrochemical devices based on CGO/Er_2O_3 multilayer microdot which allowed modulating the strain of more than 1.16% by varying the number of individual layers from 1 to 60 nm while keeping the microdot at a constant thickness [123]. Electrical measurements showed that the activation energy of the devices could be altered by 0.31 eV and the conductivity decreased by one order of magnitude [123]. Fig. 10 resume schematically the effect of strain in coherent and semi-coherent epitaxial interfaces for metal oxide oxygen conductors such as YSZ and doped CeO_2, from experimental results for biaxial strained metal oxide interface, including both single thin film and hetero-structures showing consistency with theoretical calculations.

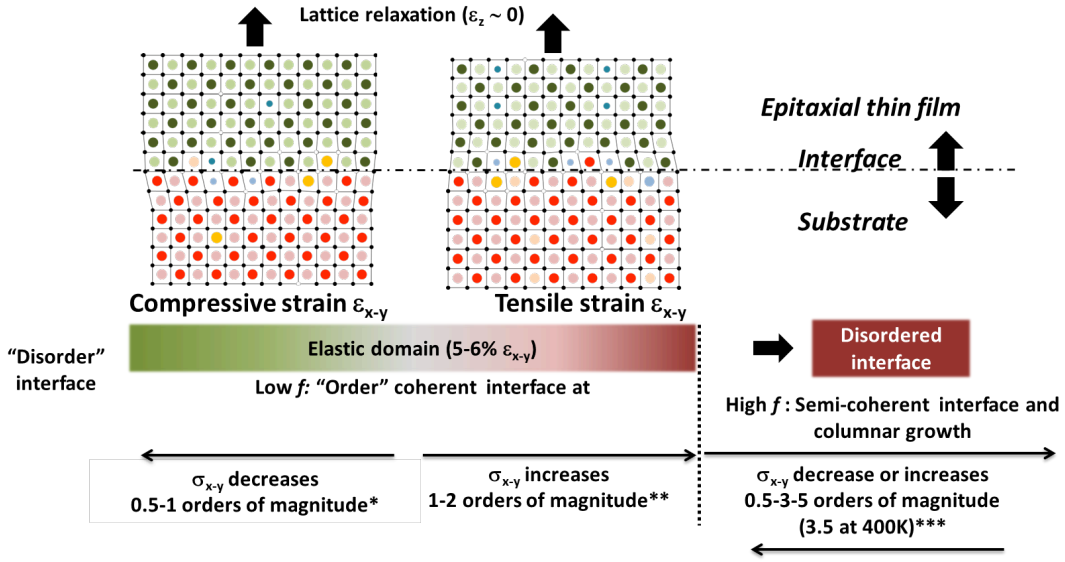

Fig. 10 Schematic representation of effect of strain at the coherent and semi-coherent interfaces: compressive stress leads to a decrease in conductivity [*101, 109, 121, 123], tensile stain lead to increase of conductivity in highly coherent [**104-108, 110-112, 117-121] and semi-coherent interfaces [***101, 112-116, 122]

New concepts: stabilization of phases and "dynamic" interfaces

Since the report on giant ionic effects were claimed in YSZ/STO, most of the work done so far on metal oxides interfaces, also discussed in this paper, has been directed towards increasing the oxygen ionic conductivity by tuning the *electro-chemo-mechanic* properties of and particularly the lattice strain effect of cubic-zirconia and doped-ceria materials. However, as also highlighted in several parts of this paper, different combinations and possibilities are accessible to control of the conductivity of metal oxide interfaces.

In our recent work, we illustrated an alternative way to use metal oxide ionic conductors interfaces in engineered heterostructure. Particularly, this was done by exploring a different concept of multi-phase material where interfaces are used to stabilize the cubic delta-phase Bi_2O_3 ionic conductor [124]. Identified more than a century ago, δ-Bi_2O_3 is recognized as one of the most technologically important oxide ion conductors with conductivity of two orders of magnitude higher than zirconia. The δ-Bi_2O_3 phase has potentially the highest known oxygen vacancy transport among the ions conductors, with $\sigma > 1$ S cm^{-1} at $T > 900$K [125]. The δ-Bi_2O_3 can be stabilized by dopants with high polarizability [126]. However, its chemical stability in low oxygen partial pressure atmosphere, *i.e.* $pO_2 < 10^{-20}$ atm, is poor and can easily react with other solids and gases, preventing using the material in real applications [125]. A feasible way to use the δ-Bi_2O_3 was pioneered by Vikar [127] and Wachsman [127], where a doped-CeO_2 layer is used together with the δ-Bi_2O_3. This strategy aims to preserve the bulk Bi_2O_3-based layer from degradation at low pO_2 [128, 129]. However, this concept is centred on a delicate balance between pO_2 and the relative thickness of the layers, and the bismuth

oxide component decomposes at low pO_2 gradients because ceria is easily reduced under low pO_2 at the CGO/Bi_2O_3 interface [127]. In our work, we developed a novel multilayer thin films made of Er_2O_3 stabilized δ-Bi_2O_3 (i.e. $Bi_{0.8}Er_{0.2}O_{2-\delta}$, ESB) and CGO, by pulsed laser deposition (PLD) on diverse substrates. The multilayer architecture is assembled at the atomic level (layer thickness ~ 2.7nm) with highly coherent interfaces, no strain effects in oxidative condition, and it is engineered to preserve the high ionic conductive δ-Bi_2O_3-phase in the CeO_2 lattice. The resulting superlattice is a composite ionic conductor, stable in a wide range of thermodynamic conditions, usually forbidden for the Bi_2O_3 δ-phase [128]. Interestingly, the multilayer thin films material show phase stability only for bismuth layers which are thinner than 10 nm and uniformly separated by CGO layers, showing that the "protective effect" of the stable material is effective only for a confinement at the nanometric scale. Conversely, for thick ESB layers the material seems to degrades, since it exposed to the low pO_2 gradients at the CGO. The nature of the lateral conductivity of such materials also presents some interesting features: (1) in oxidative conditions the heterostructure results dominantly and superior to GDC, and exhibits remarkable performance with $\sigma_{x-y} > 0.1$ S cm^{-1} for T > 500 °C; and (2) at low oxygen partial pressure (dry 9% H_2/N_2, $10^{-32} < pO_2 < 10^{-22}$ atm) the materials presents unexpected behaviour with an abrupt enhancement in conductivity. This phenomenon occurred in a short time (minutes) exhibiting a sharp transition of conductivity by increasing conductivity of two order of magnitude while preserving the same phase during the transition. Interestingly, the electrical properties across the transition were found to be stable and reversible without any traces of hysteresis in heating and cooling cycles. Investigation of different thickness ratios showed that such effect is more pronounced for samples with extremely thin CGO layers (only a few unit cells). Thick ESB films above *ca.* 10 nm degrade as also observed earlier in the bulk case [127]. The nature of the conductivity also presented interesting abrupt changes from regions of ionic to mixed ionic and electronic conductivity [124].

Beside the phase stability another feature occurring at the interface of the heterostructure was found of great interest and it could be related to the unexpected electrical performances observed in this multilayer. Ceria is known to undergo chemical expansion (*i.e.* ε_{x-y-z}) under reducing conditions, with a change in volume which, depending on the temperature and pO_2 conditions, can reach 2% of the oxidize volume [130]. Such effect is mainly driven by the change of size of the Ce-cation from Ce^{+4} (0.907 ~Å, 8-fold cubic) to Ce^{3+} (1.01 Å in 6-fold octahedral). The effect of the chemical expansion at the CGO layer in the ESB/CGO heterostructure is therefore expected to occur in reducing conditions and, due the high coherency of the materials, also to be propagated to the ESB layer via the CGO/ESB interface. This phenomenon is schematically represented in Fig. 11 as ε_{x-y} (the ε_z at CGO also occurs but it possibly is does not influence the interface). Unfortunately, the net strain at the

ESB/CGO interface is it difficult to estimate because the chemical expansion of ESB in reducing condition is still unknown. This is because the material is not stable in reducing conditions. However, large concentration and mobility of oxygen vacancies are expected in Bi-oxide under tensile strain. This is possible also by considering the variety defective configurations observed for Bi_2O_3 which possesses several phase transformations, order-disorder transitions and easy oxygen vacancies displacements [131]. In such conditions, it would be thus possible to have a sort of dynamic interface which, triggered by thermochemical factors, activate additional defects at the ESB thin layer. This fact can be potentially used to increase conductivity which, however, in this form would be accompanied by electronic effect of $Ce^{3+/4+}$ polaron hopping (see results in Fig. 11).

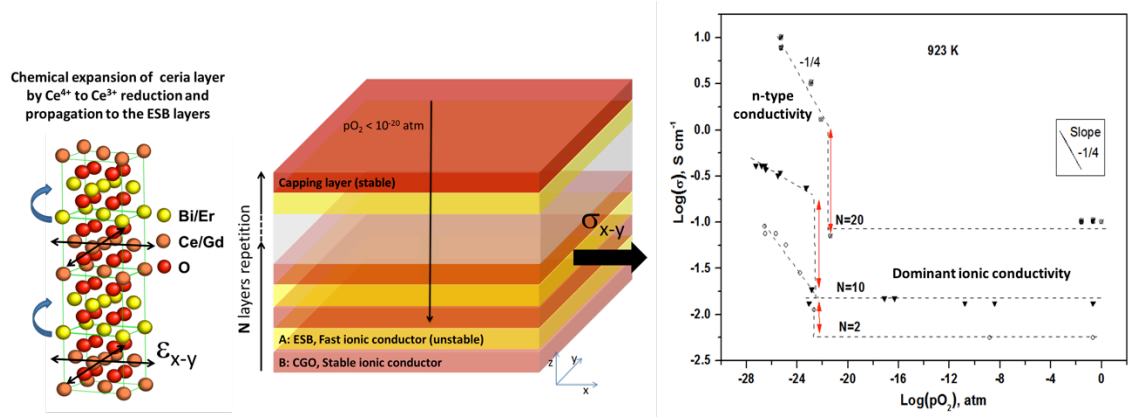

Fig. 11 Schematic representation of ESB/CGO multilayer, where interface tensile strain is possibly activated by chemical of CGO, leading to an abrupt increase in total conductivity [124]

Outlook

This approach represents a novel concept which, as also recently proposed for other defective oxides [69, 70, 123], could be already applied *e.g.* in strain-activated memristors or other applications where MIEC is desirable. However, several questions are still open and need to be answered: Is it possible to achieve oxygen super-ionic conductivity? Are the interfaces a route to enhance the conductivity? How to control elastic strain in real applications, where substrate, impurities and lattice disorder can easily affect the materials properties? Yet, how stress-induced plastic effects such as dislocation, vacancy associates, grain boundaries *etc* can be avoided or alternative controlled in real interfaces? We show that it is possible to achieve novel properties of oxide ionic conducting materials by the concepts of chemical stabilization and "dynamic strain". These, can be further leverage over the more traditional ones for further development in this field.

Overall summary:

Thin films of electronically and ionically conducting materials have opened new way to design and fabricate many miniaturized devices such as field effect transistors, fuel cells, gas sensors

etc.. Among these, oxide hetrostructures and heterointerfaces are of particular significance in creating new and novel interfacial properties often not seen in their counterpart bulk. In this review we have illustrate some of the new findings and approaches in this area and some of the challenges and scientific question which are still open and need further attention are discussed. We hope that this review will stimulate new directions in manipulating thin films and interfaces to achieve new and yet unknown properties of materials.

Acknowledgment:
This review paper is made possible through the help and support from Dr. Yunzhong Chen, and Dr. Simone Sanna. Special thanks to Mr. Dennis Christiansen and Mr. Felix Trier for providing some of the figures in this review paper.

References:

1. P. Zubko, S. Gariglio, M. Gabay, P. Ghosez, and J. M. Triscone, Interface Physics in Complex Oxide Heterostructures, Annual Review of Condensed Matter Physics Vol. 2: 141-165 (2011), DOI: 10.1146/annurev-conmatphys-062910-140445
2. R. Ramesh, Complex functional oxide heterostructures, Rcurrent Science, 105, 8, (2013) 25
3. K. Kermana and S. Ramanathan, Complex oxide nanomembranes for energy conversion and storage: A review, Journal of Materials Research, Volume 29 , Issue 03, (2014)320-337
4. J. Chakhalian, A. J. Millis and J. Rondinelli, Whither the oxide interface, Nature Materials 11, 92–94 (2012), doi:10.1038/nmat3225
5. M Yasuda, N.Akao, N. Hara, and K. Sugimoto, Self-healing corrosion protection ability of composition-gradient Al2O3 center dot Nb nanocomposite thin films. Journal of the Electrochemical Society 150, B481 (2003)
6. J. Suntivich, H. A. Gasteiger, N. Yabuuchi, H. Nakanishi, J. B. Goodenough and Y. Shao-Horn Design principles for oxygen reduction activity on perovskite oxide catalysts for fuel cells and metal-air batteries. Nature Chemistry 3, (2011) 546–550
7. T. H. DiStefano and D. E. Eastman, The Band Edge of Amorphous SiO2 by Photoinjection and Photoconductivity Measurements. Solid State Communications 9, (1971) 2259-2261
8. J. Robertson, High dielectric constant oxides. European Physical Journal - Applied Physics 28, (2004) 265-291
9. A. Schilling, M. Cantoni, J. D. Guo and H. R. Ott, Superconductivity above 130 K in the HgBaCaCuO System. Nature 363, (1993) 56-58.

10. O. N. Tufte and P. W. Chapman, Electron mobility in semiconducting strontium titanate. Physical Review 155, (1967) 796.
11. J. Maier: Nanoionics: ion transport and electrochemical storage in confined systems Nature Materials 4(11), (2005) 805-815
12. M. Grundmann, H. Frenzel, A. Lajn, M. Lorenz, F. Schein, and H. von Wenckstern, Transparent semiconducting oxides: materials and devices. Physica Status Solidi (a) - Applications and Materials Science 207, (2010) 1437-1449
13. I. Vrejoiu, G. Le Rhun, L. Pintilie, D. Hesse, M. Alexe, U. Gösele, Intrinsic ferroelectric properties of strained tetragonal PbZr0.2Ti0.8O3 obtained on layer-by-layer grown, defect-free single crystalline film. Advanced Materials 18, (2006) 1657-1661
14. S. E. Park and T. R. Shrout, Ultrahigh strain and piezoelectric behavior in relaxor based ferroelectric single crystals. Journal of Applied Physics 82, (1997) 1804-1811
15. V. K. Sergei and A. N. Morozovska, Multiferroics: Focusing light on flexoelectricity, Nature Nanotechnology 10, (2015) 916–917 doi:10.1038/nnano.2015.213
16. R. J. Soulen Jr., J. M. Byers*, M. S. Osofsky, B. Nadgorny, T. Ambrose, S. F. Cheng, P. R. Broussard, C. T. Tanaka, J. Nowak, J. S. Moodera, A. Barry, J. M. D. Coey, Measuring the spin polarization of a metal with a superconducting point contact. Science 282, (1998) 85-88
17. B. T. Matthias and R. M. Bozorth, Ferromagnetic Interaction in EuO. Physical Review Letters 7, (1961) 160-161
18. D. C. Worledge, G. J. Snyder, M. R. Beasley, T. H. Geballe, R. Hiskes and S. DiCarolis, Anneal-tunable Curie temperature and transport of La0.67Ca0.33MnO3. Journal of Applied Physics 80, (1996) 5158-5161
19. A. Maignan, C.Simon, V.Caignaert and B. Raveau, Giant Magnetoresistance Ratios Superior to 10^{11} in Manganese Perovskites. Solid State Communications 96, (1995) 623-625
20. R. M. Bozorth, E. F. Tilden and A. J. Williams, Anisotropy and Magnetostriction of some Ferrites. Physical Review 99, (1955) 1788-1798
21. A. Rijnders, G. Koster, D. H. A. Blank, and H. Rogalla, In-situ monitoring during pulsed laser deposition of complex oxides using reflection high energy electron diffraction under high oxygen pressure. Appl. Phys. Lett. **70**, (1997) 1888
22. H.Kroemer, Nobel Lecture: Quasielectric fields and band offsets: teaching electrons new tricks. Review of Modern Physics 73 , (2001) 783-793
23. Editorial, The interface is still the device. Nature Mater. 11, (2012) 91
24. C. Richter, H. Boschker, W. Dietsche, E. Fillis-Tsirakis, R. Jany, F. Loder, L. F. Kourkoutis, D. A. Muller, J. R. Kirtley, C. W. Schneider and J. Mannhart, Interface

superconductor with gap behaviour like a high-temperature superconductor. Nature 502, (2013) 528

25. H. Ohta, S. W. Kim, Y. Mune, T. Mizoguchi, K. Nomura, S. Ohta, T. Nomura, Y. Nakanishi, Y. Ikuhara, M. Hirano, H. Hosono and K. Koumoto, Giant thermoelectric Seebeck coefficient of a two-dimensional electron gas in $SrTiO_3$. Nature Mater. **6**, (2007) 129
26. J. Garcia-Barriocanal, A. Rivera-Calzada, M. Varela, Z. Sefrioui, E. Iborra, C. Leon, S. J. Pennycook, J. Santamaria,, Colossal Ionic Conductivity at Interfaces of Epitaxial ZrO2:Y2O3/SrTiO3 Heterostructures. Science 321, (2008) 676
27. A. Brinkman, M. Huijben, M. van Zalk, J. Huijben, U. Zeitler, J. C. Maan, W. G. van der Wiel, G. Rijnders, D. H. A. Blank and Hilgenkamp, Magnetic effects at the interface between non-magnetic oxides. Nature Mater. 6, (2007) 493
28. A. Ohtomo and H. Y. Hwang, A high-mobility electron gas at the LaAlO3/SrTiO3 heterointerface, Nature 427, (2004) 423
29. C. Cen, S. Thiel, J. Mannhart, J. Levy, Oxide Nanoelectronics on Demand, Science 323, (2009) 1026
30. Y. Lei, Y. Li, Y. Z. Chen, Y. W. Xie, Y. S. Chen, S. H. Wang, J. Wang, B. G. Shen, N. Pryds, H. Y. Hwang, and J. R. Sun. Visible light-enhanced gating effect at LaAlO3/SrTiO3 interface. Nature Commun. 5, (2014) 5554
31. S. Thiel, G. Hammerl, A. Schmehl, C. W. Schneider and J. Mannhart, Tunable quasi-two dimensional electron gases in oxide heterostructures. Science 313 (2006) 1942-1945.
32. Y. Z. Chen, N. Pryds, J. E. Kleibeuker, J. R. Sun, E. Stamate, G. Koster, B. G. Shen, G. Rijnders, and S. Linderoth 'Metallic and insulating interfaces of amorphous SrTiO3-based oxide heterostructures'. Nano. Lett. 11, (2011) 3774
33. Y. Kozuka, M. Kim1, H. Ohta, Y. Hikita, C. Bell1, and H. Y. Hwang 'Enhancing the electron mobility via delta-doping in SrTiO3', Appl. Phys. Lett. 97, (2010) 222115
34. O. N. Tubate and P.W. Chapman, Elelctron Mobility in Semiconducting Strontium Titanate, Physical Review, 155, 3 (1967) 15.
35. H. E. Weaver, Dielectric properties of single crystals of SrTiO3 at low temperatures, J. Phys. Chem. Solids 11, (1959) 274
36. K. A. Müller, W. Berlinger, and F. Waldner, Characteristic Structural Phase Transition in Perovskite-Type Compounds, Phys. Rev. Lett. 21 (1968) 814–17
37. K. A. Müller and H. Burkard, SrTiO3: An intrinsic quantum paraelectric below 4 K, Phys. Rev. B.19, (1979) 3593
38. Y. Z. Chen, N. Bovet, F. Trier, D. V. Christensen, F. M. Qu, N. H. Andersen, T. Kasama, W. Zhang, R. Giraud, J. Dufouleur, T. S. Jespersen, J. R. Sun, A. Smith, J.

Nygård, L. Lu, B. Büchner, B. G. Shen, S. Linderoth and N. Pryds, A high-mobility two-dimensional electron gas at the spinel/perovskite interface of γ-Al2O3/SrTiO3. Nature Commun. 4, (2013) 1371

39. Y. Chen, F. Trier, T. Kasama, D. V. Christensen, N. Bovet, Z. I. Balogh, H. Li, K. T. S. Thydén, W. Zhang, S. Yazdi, P. Norby, N. Pryds, and S. Linderoth, Creation of high mobility two-dimensional electron gases via strain induced polarization at an otherwise nonpolar complex oxide interface. Nano Lett., 15 (3) (2015) 1849
40. Y. Z. Chen, F. Trier, T. Wijnands, R. J. Green, N. Gauquelin, R. Egoavil, D. V. Christensen, G. Koster, M. Huijben, N. Bovet, S. Macke, F. He, R. Sutarto, N. H. Andersen, J. A. Sulpizio, M. Honig, G. E. D. K. Prawiroatmodjo, T. S. Jespersen, S. Linderoth, S. Ilani, J. Verbeeck, G. Van Tendeloo, G. Rijnders, G. A. Sawatzky and N. Pryds, Extreme mobility enhancement of two-dimensional electron gases at oxide interfaces by charge-transfer-induced modulation doping, Nature Materials. 14 (2015) 801 10.1038/nmat4303
41. R. Jany, C. Richter, C. Woltmann, G. Pfanzelt, B. Förg, M. Rommel, T. Reindl, U. Waizmann, J. Weis, J. A. Mundy, D. A. Muller, H. Boschker, J. Mannhart, Monolithically Integrated Circuits from Functional Oxides. Adv. Mater. Interfaces, 1 (2014)1300031. doi: 10.1002/admi.201300031
42. R. Dingle, Electron Mobility in Modulation-doped semiconductor hetrojunction superlattices. Appl. Phys. Lett., 33, (1978) 665
43. C. Cen, S. Thiel, G. Hammerl, C. W. Schneider, K. E. Andersen, C. S. Hellberg, J. Mannhart and J. Levy, Nanoscale control of an interfacial metal-insulator transition at room temperature. Nature Mater. 7, (2008) 298
44. F. Bi, Daniela F. Bogorin, C. Cen, C. W. Bark, J. W. Park, C. B. Eom and J. Levy, "Water-cycle" mechanism for writing and erasing nanostructures at the LaAlO3 /SrTiO3 interface. Applied Physics Letters 97 , (2010) 173110
45. D. V. Christensen, F. Trier, Y. Z. Chen, A. Smith, J. Nygård, and N. Pryds. Controlling interfacial states in amorphous/crystalline LaAlO3/SrTiO3 heterostructures by electric fields. Appl. Phys. Lett. 102 (2013) 021602
46. Y. Z. Chen, J. L. Zhao, J. R. Sun,N. Pryds and B. G. Shen,: Resistance Switching at the interface of LaAlO3/SrTiO3, Appl. Phys. Lett., 97, (2010) 1
47. A. Tsukazaki, A. Ohtomo, T. Kita, Y. Ohno, H. Ohno, M. Kawasaki, Quantum Hall Effect in Polar Oxide Heterostructures, Science 315, (2007) 1388–1391
48. A. Tsukazaki, S. Akasaka, K. Nakahara, Y. Ohno, H. Ohno, D. Maryenko, A. Ohtomo and M. Kawasaki, Observation of the fractional quantum Hall effect in an oxide, Nature Mater. 9, (2010) 889-893

49. M. Gabay and J. M. Triscone, Oxide heterostructures: Hund rules with a twist, Nature Phys. 9, (2013) 610
50. Trier, et al., Quantum Hall effect at a SrTiO3-based heterointerface: evidence of a multiple quantum well nature, Nature Physics (submitted)
51. M. Breitschaft, V. Tinkl, N. Pavlenko, S. Thiel, C. Richter, J. R. Kirtley, Y. C. Liao, G. Hammerl, V. Eyert, T. Kopp, J. Mannhart, Two-dimensional electron liquid state at LaAlO3-SrTiO3 interfaces, PRB 81, (2010) 153414
52. J. A. Sulpizio, S. Ilani, P. Irvin, J. Levy, Nanoscale Phenomena in Oxide Heterostructures, Annu. Rev. Mater. Res. 44 (2014) 117–49
53. B. Kalisky, E. M. Spanton, H. Noad, J. R. Kirtley, K. C. Nowack, C. Bell, H. K. Sato, M. Hosoda, Y. Xie, Y. Hikita, C. Woltmann, G. Pfanzelt, R. Jany, C. Richter, H. Y. Hwang, J. Mannhart and K. A. Moler, Locally enhanced conductivity due to the tetragonal domain structure in LaAlO3/SrTiO3 heterointerfaces, Nature Materials, 12, 1091 (2013)
54. Z. Q. Liu, D. P. Leusink, X. Wang, W. M. Lü, K. Gopinadhan, A. Annadi, Y. L. Zhao, X. H. Huang, S. W. Zeng, Z. Huang, A. Srivastava, S. Dhar, T. Venkatesan, and Ariando, Metal-Insulator Transition in SrTiO3-x Thin Films Induced by Frozen-Out Carriers, PRL 107, (2011) 146802
55. J. Biscaras, N. Bergeal, A. Kushwaha, T. Wolf, A. Rastogi, R.C. Budhani and J. Lesueur, Two-dimensional superconductivity at a Mott insulator/band insulator interface LaTiO3/SrTiO3, Nat. Commun. 1 (2010) 89
56. P. Perna, D. Maccariello, M. Radovic, U. Scotti di Uccio, I. Pallecchi, M. Codda, D. Marré, C. Cantoni, J. Gazquez, M. Varela, S. J. Pennycook and F. Miletto Granozio, Conducting interfaces between band insulating oxides: the LaGaO3/SrTiO3, Appl. Phys. Lett. 97 (2010) 152111
57. K. Shibuya, T. Ohnishi, M. Lippma and M. Oshima, Metallic conductivity at the CaHfO3/ SrTiO3 interface, Appl. Phys. Lett. 91 (2007) 232106
58. M. Huijben, G. Koster, M. K. Kruize, S. Wenderich, J. Verbeeck, S. Bals, E. Slooten, B. Shi, H. J. A. Molegraaf, J. E. Kleibeuker, S. van Aert, J. B. Goedkoop, A. Brinkman, D. H. A. Blank, M. S. Golden, G. van Tendeloo, H. Hilgenkamp, G. Rijnders, Defect Engineering in Oxide Heterostructures by Enhanced Oxygen Surface Exchange, Adv. Funct. Mater., 23 (2013) 5240–5248
59. D.H. Whitmore. Ionic and Mixed Conductors for Energy Storage and Conversion Systems. J Cryst Growth, **39**, 160–179 (1976)
60. P. Knauth, H.L. Tuller, Solid-State Ionics: Roots, Status, and Future Prospects, J. Am. Ceram. Soc. **85 (7)**, 1654–1680 (2002)

61. H.L. Tuller, Ionic conduction in nanocrystalline materials, Solid State Ionics, **131**, 143–157 (2000)
62. A.S. Aricò, P. Bruce, B. Scrosati, J.-M. Tarascon, W. van Schalkwijk. Nanostructured materials for advanced energy conversion and storage devices, Nat. Mater. **4**, 366 – 377 (2005)
63. J. Maier. Nanoionics: ion transport and electrochemical storage in confined systems. Nat. Mater, **4**, 805 – 815 (2005)
64. N.Q. Minh, Ceramic Fuel Cells, J. Am. Ceram. Soc, 76(3), 563–588 (1993)
65. SM Haile. Fuel Cell Materials and Components. Acta Mater, **51**(19), 5981–6000 (2003)
66. A. Aguadero, L. Fawcett, S. Taub, R. Woolley, K.-T. Wu, N. Xu, J.A. Kilner, S.J. Skinner, Materials development for intermediate-temperature solid oxide electrochemical devices. J. Mater. Sci. 47(9), 3925–3948 (2012)
67. A. Trovarelli, Catalytic Properties of Ceria and CeO2-Containing Materials, Catal. Rev.: Sci. Eng. **38(4)**, 439-520 (1996)
68. Oudenhoven, J. F. M., Baggetto, L. & Notten, P. H. L. All-solid-state lithium-ion microbatteries: A review of various three-dimensional concepts. Adv. Energy Mater. **1**, 10-33 (2011)
69. Waser, R., Dittmann, R., Staikov, G. & Szot, K. Redox-based resistive switching memories - nanoionic mechanisms, prospects, and challenges. Adv. Mater. 21, 2632_2663 (2009)
70. Messerschmitt, F., Kubicek, M., Schweiger, S. & Rupp, J. L. M. Memristor kinetics and di_usion characteristics for mixed anionic-electronic SrTiO3-d bits: The memristor-based cottrell analysis connecting
71. T.-M. Chiang, D. Birnie III, W.D. Kingery, Physical Ceramics: Principles for Ceramic Science and Engineering, MIT series in materials science and Enginering Chap 3, John Wiley 6 Sons, 1997: ISBN 0-471-59873-9
72. J.E. Bauerle, Study of solid electrolyte polarization by a complex admittance method, J. Phys. Chem, Solids, 30, 2657-2670 (1969)
73. S. Kim, J. Maier, On the Conductivity Mechanism in Nanocrystalline Ceria, J. Electrochem. Soc. 149 (19), J73-J83 (2002)
74. J. Maier, Pushing Nanoionics to the Limits: Charge Carrier Chemistry in Extremely Small Systems, Chem. Mater. 26, 348-360 (2014)
75. Schoonman, J. "Nanoionics." Ed. by J. Molenda. Solid State Ionics, Solid State Ion, Sol St Ion, Solid State Ionics, Solid State Ionics Diffusion and Reactions 157.1-4 (2003): 319–326

76. Cai, Z., Kuru, Y., Han, J. W., Chen, Y. & Yildiz, B. Surface electronic structure transitions at high temperature on perovskite oxides: the case of strained La0.8Sr0.2CoO3 thin films. J. Am. Chem. Soc. 133, 17696–17704 (2011)
77. Kubicek, M. et al. Tensile lattice strain accelerates oxygen surface exchange and diffusion in La1_xSrxCoO3_d thin films. ACS Nano 7, 3276–3286 (2013)
78. Hong, W. T. et al. Tuning the spin state in LaCoO3 thin films for enhanced high-temperature oxygen electrocatalysis. J. Phys. Chem. Lett. 4, 2493–2499 (2013)
79. J.L.M. Rupp, Ionic diffusion as a matter of lattice-strain for electroceramic thin films, Solid State Ionics 207, 1-13 (2012)
80. K. Lehovec, "Space Charge Layer and Distribution of Lattice Defects at theSurface of Ionic Crystals," J. Chem. Phys., 21, 1123–28 (1953)
81. K. L. Kliewer and J. S. Koehler, "Space Charge in Ionic Crystals. I. GeneralApproach with Application to NaCl," Phys. Rev., 140, 1226–40 (1965)
82. B. Poeppel and J. M. Blakely, "Origin of Equilibrium Space Charge Potentialsin Ionic Crystals," Surf. Sci., 15, 507–23 (1969)
83. S. Hull, Superionics: crystal structures and conduction processes, Rep. Progr. Phys, 67(7), 1233-1314 (2004)
84. J.S. Lee, D.-Y Kim, Space-charge concepts on grain boundary impedance of a high-purity yttria-stabilized tetragonal zirconia polycrystal. J. Mater. Res. 16 (9), 2739-2751 (2001)
85. R. A. De Souza, J. Fleig, J. Maier, O. Kienzle, Z.L. Zhang, W. Sigle, M. Ruhle. Electrical and structural characterization of a low-angle tilt grain boundary in iron-doped strontium titanate. J. Am. Ceram. Soc, **86(6)**, 922–928 (2003)
86. P.Thongbai, S. Tangwancharoen, T. Yamwong.. Dielectric relaxation and dielectric response mechanism in (Li, Ti)-doped NiO ceramics. J. Phys.: Cond. Matter, **20(39)**, 395227 (1-11) (2008)
87. A. Atkinson, Surface and interface mass transport in ionic materials, Solid State Ionics, 28-30, 1377-1387 (1988)
88. B.J. Wuensch and H.L. Tuller, Lattice diffusion, grain boundary diffusion and defect structure of ZnO, J. Phys. Chem. Sol., **55(10)**, 975-984 (1994)
89. P. Knauth, Ionic Conductor Composites: Theory and Materials, J. Electroceram. **5:2**, 111-125 (2000)
90. S. Kim, J. Fleig, J. Maier. Space charge conduction: Simple analytical solutions for ionic and mixed conductors and application to nanocrystalline ceria. Phys. Chem. Chem. Phys. **5(11)**, 2268–2273 (2003)
91. D.C. Brydges,; Ph.A. Martin. Coulomb Systems at Low Density: A Review. J. Stat. Phys. **96 (5/6)**,1163–1330. (1999)

92. A. Tschöpe, Grain size-dependent electrical conductivity of polycrystalline cerium oxide II: Space charge model, Solid State Ionics **139**, 267–280 (2001)
93. V. Esposito, E. Traversa, Design of Electroceramics for Solid Oxides Fuel Cell Applications: Playing with Ceria, J. Am. Ceram. Soc., **91 [4]**, 1037–1051 (2008)
94. V. Esposito, D.W. Ni, Z. He, W. Zhang, A.S. Prasad, J.A. Glasscock, C. Chatzichristodoulou, S. Ramousse, A. Kaiser, Enhanced mass diffusion phenomena in highly defective doped ceria, Acta Mater. **61**, 6290–6300 (2013)
95. D. W. Ni, D. Z. de Florio, D. Marani, A. Kaiser, V. B. Tinti, V. Esposito. Effect of chemical redox on Gd-doped ceria mass diffusion, *J. Mater. Chem. A*, **3**, 18835-18838 (2015)
96. A. Evans, A. Bieberle-Hütter, J. L. M. Rupp, L.J. Gauckler. Review on microfabricated micro-solid oxide fuel cell membranes. J. Power Sources **194**, 119–129 (2009)
97. F. D'Heurle, J. Harper. Note on the origin of intrinsic stresses in films deposited via evaporation and sputtering. Thin Solid Films **171**, 81–92 (1989)
98. K. Kerman, T. Tallinen, S. Ramanathan, L. Mahadevan. Elastic configurations of self-supported oxide membranes for fuel cells. J. Power Sources 222, 359–366 (2013)
99. M. G. Blamire, J. L. MacManus-Driscoll, N. D. Mathur, Z. H. Barber. The Materials Science of Functional Oxide Thin Films. Adv. Mater. **21**, 3827 (2009)
100. X. Guo, Can we achieve significantly higher ionic conductivity in nanostructured zirconia? Scripta Mater. **65**, 96–101 (2011)
101. C. Korte, J. Keppner, A. Peters, N. Schichtel, H. Aydin, J. Janek. Coherency strain and its effect on ionic conductivity and diffusion in solid electrolytes – an improved model for nanocrystalline thin films and a review of experimental data, Phys. Chem. Chem. Phys.**16**, 24575-24591 (2014)
102. S. Giraud, J. Canel, Young's modulus of some SOFCs materials as a function of temperature. J. Eur. Ceram. Soc, **28(1)**, 77–83 (2008)
103. A. Cavallaro, M. Burriel, J. Roqueta, A. Apostolidis, A. Bernardi, A. Tarancón, R. Srinivasan, S. N. Cook, H. L. Fraser, J. A. Kilner, D. W. McComb, J. Santiso, Electronic nature of the enhanced conductivity in YSZ-STO multilayers deposited by PLD. Solid State Ionics. 181, 592–601 (2010)
104. Y. Shi, A.H. Bork, S. Schweiger, J.L.M. Rupp. The effect of mechanical twisting on oxygen ionic transport in solid-state energy conversion membranes, Nat. Mater, 14, 721-728 (2015)
105. J. G. Swallow, W.H. Woodford, Y. Chen, Q. Lu, J.J. Kim, D. Chen, Y.-M. Chiang, W.C. Carter, B. Yildiz, H. L. Tuller, K. J. Van Vliet. Chemomechanics of

ionically conductive ceramics for electrical energy conversion and storage, J Electroceram, **32(1)**, 3-27 (2014)

106. R. De Souza, A. Ramadan, S. Hörner. Modifying the barriers for oxygen-vacancy migration in fluorite-structured CeO2 electrolytes through strain: a computer simulation study. Energy Environ. Sci. **5**, 5445-53 (2012)

107. N. Schichtel, C. Korte, D. Hesse and J. Janek. Elastic strain at interfaces and its influence on ionic conductivity in nanoscaled solid electrolyte thin films—theoretical considerations and experimental studies, Phys. Chem. Chem. Phys. **11**, 3043-3048 (2009)

108. A. Kushima and B. Yildiz, Oxygen ion diffusivity in strained yttria stabilized zirconia: where is the fastest strain? J. Mater. Chem. **20**, 4809-4819 (2010)

109. J. A. Hirschfeld, H. Lustfeld. First-principles study and modeling of strain-dependent ionic migration in ZrO2. Phys. Rev. B **84**, 224308(1-7) (2011)

110. J. A. Hirschfeld, H. Lustfeld, Enhanced anisotropic ionic diffusion in layered electrolyte structures from density functional theory, Phys. Rev. B **89**, 014305 (1-5) (2014)

111. M. Burbano, D. Marrocchelli, G.W. Watson. Strain effects on the ionic conductivity of Y-doped ceria: A simulation study, J. Electroceram. **32**, 28–36 (2014)

112. S.D. Aidhy, Y. Zhang, W.J. Weber. Strained Ionic Interfaces: Effect on Oxygen Diffusivity from Atomistic Simulations. J. Phys. Chem. C 118, 4207–4212 (2014)

113. L. Sun, D. Marrocchelli, Y.B. Yildiz. Edge dislocation slows down oxide ion diffusion in doped CeO2 by segregation of charged defects, Nat Comm. 6, 6294, 82015) doi:10.1038/ncomms7294

114. B. Li , J.M. Zhang , T. Kaspar , V. Shutthanandan , R.C. Ewing , J. Lian. Multilayered YSZ/GZO films with greatly enhanced ionic conduction for low temperature solid oxide fuel cells. Phys. Chem. Chem. Phys. 15 (4), 1296-1301 (2013)

115. A. Chroneos, B. Yildiz, A. Tarancón, D. Parfitta, J.A. Kilner, Oxygen diffusion in solid oxide fuel cell cathode and electrolyte materials: mechanistic insights from atomistic simulations, Energy Environ. Sci. 4, 2774-2789 (2011)

116. M. Sillassen, P. Eklund, N. Pryds, E. Johnson, U. Helmersson, J. Bøttiger, Low-Temperature Superionic Conductivity in Strained Yttria-Stabilized Zirconia, Adv. Funct. Mater. **20**, 2071–2076 (2010)

117. K. M. Kant, V. Esposito, N. Pryds, Strain induced ionic conductivity enhancement in epitaxial Ce0.9Gd0.1O2−δ thin films. Appl. Phys. Lett. **100**, 033105 (2012)

118. K.M. Kant, V. Esposito, N. Pryds. Enhanced conductivity in pulsed laser deposited Ce0.9Gd0.1O2−_ /SrTiO3 heterostructures, Appl. Phys Lett. 97, 143110 (1-3) (2010)

119. S. Sanna, V. Esposito, D. Pergolesi, A. Orsini, A. Tebano, S. Licoccia, G. Balestrino, E. Traversa. Fabrication and Electrochemical Properties of Epitaxial Samarium-Doped Ceria Films on SrTiO3-Buffered MgO Substrates, Adv. Funct. Mater. **19**, 1–7 (2009)

120. S. Sanna, V. Esposito, A. Tebano, S. Licoccia, E. Traversa and G. Balestrino, Enhancement of Ionic Conductivity in Sm-Doped Ceria/Yttria-Stabilized Zirconia Heteroepitaxial Structures. Small. **6**, 1863–1867 (2010)

121. H. Aydin, C. Korte,M. Rohnke, J. Janek, Oxygen tracer diffusion along interfaces of strained Y2O3/YSZ multilayers. Phys. Chem. Chem. Phys. 15, 1944–1955 (2013)

122. D. Pergolesi, E. Fabbri, S.N. Cook, V. Roddatis, E. Traversa, J.A. Kilner, Tensile lattice distortion does not affect oxygen transport in yttria-stabilized zirconia–CeO2 heterointerfaces. ACS Nano 6, 10524–10534 (2012)

123. S. Schweiger, M. Kubicek, F. Messerschmitt, C. Murer, L.M.Rupp Jennifer L. M. Rupp. A Microdot Multilayer Oxide Device: Let Us Tune the Strain-Ionic Transport Interaction, ACS Nano, **8** (5), pp 5032–5048 (2014)

124. S. Sanna, V. Esposito, J. Andreasen, J. Hjelm, W. Zhang,T. Kasama, S.B. Simonsen, M. Christensen, S. Linderoth, N. Pryds, Enhancement of the chemical stability in confined δ-Bi2O3, Nat. Mater. 14, 500–504 (2015)

125. E.D. Wachsman, K.T. Lee. Lowering the temperature of solid oxide fuel cells. Science **334**, 935–939 (2011)

126. P.D. Battle, C.R.A. Catlow, J.W. Heap, L.M. Moroney Structural and dynamical studies of δ-Bi_2O_3 oxide-ion conductors II. A structural comparison of $(Bi_2O_3)_{1-x}(M_2O_3)_x$ for M = Y, Er and Yb. J. Solid State Chem. **67**, 42–50 (1987)

127. A.V. Virkar, Theoretical Analysis of Solid Oxide Fuel Cells with Two-Layer, Composite Electrolytes: Electrolyte Stability, J. Electrochem. Soc. 138 (5) 1481-1487 (1991)

128. E.D. Wachsman, G.R. Ball, N. Jiang, D.A. Stevenson. Structural and defect studies in solid oxide electrolytes. Solid State Ionics 52 (1), 213-218 (1992)

129. J.Y. Park, H. Yoon, E.D. Wachsman, Fabrication and characterization of high-conductivity bilayered electrolytes for intermediate-temperature solid oxide fuel cells. J. Am. Ceram. Soc. **88**, 2402–2408 (2005)

130. D.W. Ni, J.A. Glasscock, A. Pons, W. Zhang, A. Prasad, S. Sanna, N. Pryds, V. Esposito, Densification of Highly Defective Ceria by High Temperature Controlled Re-Oxidation. J. Electrochem. Soc., 161 (11) F3072-F3078 (2014)

131. M.J. Verkerk, G.M.H. Velde, A.J. van de Burggraaf, R.B. Helmholdt, Structure and ionic conductivity of Bi2O3 substituted with lanthanide oxides. J. Phys Chem. Solids, **43(12)**, 1129-1136 (1982)